Journal of Power Sources 237 (2013) 229–242

Contents lists available at SciVerse ScienceDirect

Journal of Power Sources

journal homepage: www.elsevier.com/locate/jpowsour

Review

Recent progress in high-voltage lithium ion batteries

Meng Hu, Xiaoli Pang, Zhen Zhou*

Tianjin Key Laboratory of Metal and Molecule Based Material Chemistry, Key Laboratory of Advanced Energy Materials Chemistry (Ministry of Education), Institute of New Energy Material Chemistry, Nankai University, Tianjin 300071, China

HIGHLIGHTS

- The progress is summarized for cathode materials in high-voltage Li ion batteries.
- The development in high-voltage electrolytes is particularly reviewed, as well as other cell components.
- Also, the challenges and prospects of high-voltage Li ion batteries are discussed.

GRAPHICAL ABSTRACT

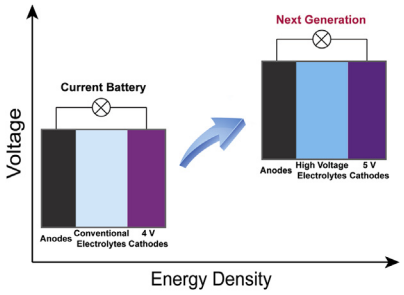

ARTICLE INFO

Article history:
Received 31 January 2013
Received in revised form
1 March 2013
Accepted 5 March 2013
Available online 9 April 2013

Keywords:
Lithium ion battery
High voltage
Cathode
Electrolyte
Additive

ABSTRACT

The energy density of Li ion batteries (LIBs) needs to be improved for the requirement of electric vehicles, hybrid electric vehicles and smart grids. Developing high-voltage LIBs is an important trend. In recent years, high-voltage cathode materials, such as $LiCoPO_4$, $Li_3V_2(PO_4)_3$, Li_2CoPO_4F, $LiNi_{0.5}Mn_{1.5}O_4$, and lithium-rich layered oxides, and matched electrolytes including stable solvents and functional additives, have been investigated extensively. In this review, we summarize the recent progress in high-voltage cathode materials and matched electrolytes, as well as the optimization of other cell components such as conductive agents, binders, positive cans, separators and current collectors. The problems and prospects of high-voltage LIBs are also discussed.

1. Introduction

Energy plays an important part in the development of modern society. The traditional fossil fuels could not meet the requirements of the rapid development of global economy gradually. Meanwhile, the combustion of fossil fuels brings air pollution and greenhouse effect [1]. Extensive investigations have been taken on the exploitation of new energy sources, such as solar, wind, tidal, and geothermal energy. However, these energy sources are instable in time and space, and require to be applied after appropriate conversion and storage [2]. Lithium ion batteries (LIBs) have been the most efficient energy storage devices since their commercialization, with the characteristics of high open-circuit voltage, large discharge capacity, long cycle life and environmental friendliness. LIBs have been widely applied to portable electronic devices and will have more extensive application prospects in electric vehicles (EVs), hybrid EVs (HEVs) and smart grids [3].

The performances of LIBs highly depend on the structure and properties of the active electrode materials and electrolytes, especially the characteristics of cathode materials. $LiCoO_2$ is the

* Corresponding author. Tel.: +86 22 23503623; fax: +86 22 23498941.
E-mail address: zhouzhen@nankai.edu.cn (Z. Zhou).

0378-7753/$ – see front matter © 2013 Elsevier B.V. All rights reserved.
http://dx.doi.org/10.1016/j.jpowsour.2013.03.024

dominant cathode material currently, which provides an energy density of ~150 Wh kg^{-1}. However, $LiCoO_2$ is undesirable to be applied in the field of EVs and HEVs due to the low energy density and the drawbacks of high cost and safety concern [4]. Great efforts have been made for two decades to develop cathode materials with high discharge voltage platforms and large capacities to improve the energy density of LIBs. Up to now, the most studied cathode materials include three types, poly-anion oxides, spinel-type oxides, and α-$NaFeO_2$-type layered oxides, and the representatives are $LiFePO_4$, $LiMn_2O_4$, and $LiNi_xCo_yMn_{1-x-y}O_2$, respectively [5]. However, the practical capacities of these materials are comparable to or only slightly higher than those of commercial $LiCoO_2$. Since the mass energy density is the product of discharge capacity and average discharge voltage, it is critical to search for materials with high discharge voltage plateaus, which can provide much more room to improve the energy density [6].

The high-voltage cathode materials that have been reported are summarized in Table 1, most of which are based on the above three types of materials. Polyanionic cathode materials have been extensively investigated since Padhi et al.'s report [32], which mainly include phosphates (such as olivine $LiMPO_4$, and monoclinic $Li_3M_2(PO_4)_3$) [33–36], pyrophosphates [37], fluorophosphates [38–40], borates $LiMBO_3$ [41], tavorite fluorosulphates $LiMSO_4F$ [42], and orthosilicates Li_2MSiO_4 [43]. The olivine phosphates ($LiMPO_4$) exhibit moderate theoretical discharge capacity, high thermodynamic stability, and stable discharge platform. The redox potentials are 3.5, 4.1, 4.8, and 5.1 V (vs. Li/Li^+) when M = Fe, Mn, Co, and Ni, respectively [8]. $LiFePO_4$ is particularly remarkable due to its good cyclic performance, abundant raw materials, non-toxicity, etc. However, the lower discharge plateau leads to lower energy density compared with $LiCoO_2$. Due to the low packing density of phosphate composites with electrically conductive substances such as carbon, the decrease in volumetric energy density is further enlarged [4]. The introduction of $V^{3+/4+/5+}$, $Co^{2+/3+}$ and $Ni^{2+/3+}$ couples ($Li_3V_2(PO_4)_3$, $LiCoPO_4$, Li_2CoPO_4F, $LiNiPO_4$, etc) could increase the discharge plateaus and the energy density noticeably. For spinel oxide $LiMn_2O_4$, the discharge plateau could also be improved by replacing Mn partly with other transition metal ions with high potential couples ($Ni^{2+/3+/4+}$, $Cr^{3+/4+}$, $Co^{3+/4+}$, etc). The discharge potentials of layered oxides $LiNi_xCo_yMn_{1-x-y}O_2$ are unlikely to be improved remarkably due to the restriction of $Ni^{2+/3+/4+}$ and $Co^{3+/4+}$ couples. However, the composites of $LiNi_xCo_yMn_{1-x-y}O_2$ and Li_2MnO_3 exhibit super large capacities (>300 mAh g^{-1}) and high energy densities under high charge/discharge cutoff voltages (above 4.5 V) [30], which are also the candidate cathode materials for high-voltage LIBs. Meanwhile, developing electrolytes with high anodic stability and excellent Li^+ diffusion kinetics is another key task to build high-voltage LIBs. The serious decomposition of carbonate electrolytes on the cathode surfaces degrades the performance of high-voltage cathodes. Besides, the instability of electrolytes under high voltages will cause storage problems and safety issues.

Very recently, Kraytsberg and Ein-Eli [6] have summarized the achievements and challenges in 5 V cathode materials for LIBs. In the present review, we will systematically discuss the recent progress in high-voltage LIBs, including the promising candidates of high-voltage cathode materials based on the dominant three structural types, high-voltage electrolyte solvents and additives, as well as their optimizations. The developments of other components in full cells, such as conductive agents, binders, positive cans, separators and current collectors, will also be involved. The challenges and prospects of high-voltage LIBs will be analyzed finally.

2. High-voltage cathode materials

Though various Co or Ni based polyanionic cathode materials exhibit high electrode potentials (such as phosphates, sulfates and silicates in Table 1), most of them (except phosphates and fluorophosphates) are rarely reported due to the difficult synthesis and the infant research stage. Therefore, in this section we mainly summarize the high-voltage cathode materials based on phosphates and fluorophosphates, spinels, and Li-rich layered oxides. For the involved cathode materials below, some are authentically high-voltage cathode materials with average discharge potential of even ~5 V (vs. Li/Li^+), and others essentially present moderate average discharge potentials. We still include the latter ones in this section since they exhibit high specific capacities only when they are charged to high potentials. For example, $Li_3V_2(PO_4)_3$ gives a theoretical discharge capacity of 197 mAh g^{-1}, when three Li ions

Table 1
Electrochemical data of high-voltage cathode materials.

	Average discharge potential [V (vs. Li/Li^+)]	Redox couple[a]	Theoretical capacity [mAh g^{-1}]	Potential range [V (vs. Li/Li^+)]	Refs
$LiCoPO_4$	4.8	$Co^{2+/3+}$	167	3.0–5.1	[7]
$LiNiPO_4$	~5.1	$Ni^{2+/3+}$	167	3.0–5.5	[8]
$Li_3V_2(PO_4)_3$	3.8	$V^{3+/4+/5+}$	197	3.0–4.8	[9]
$Li_2CoP_2O_7$	4.9	$Co^{2+/3+}$	109[b]	2.0–5.5	[10]
$Li_2MnP_2O_7$	4.45	$Mn^{2+/3+}$	110[b]	2.0–4.7	[11]
Li_2CoPO_4F	~4.9	$Co^{2+/3+}$	143[b]	3.0–5.5	[12,13]
Li_2NiPO_4F	~5.1	$Ni^{2+/3+}$	143[b]	3.0–5.5	[14]
$LiCoSO_4F$	4.7–4.9[c]	$Co^{2+/3+}$	149	–	[15–17]
$LiNiSO_4F$	5.2–5.4[c]	$Ni^{2+/3+}$	149	–	[15–17]
$LiCuSO_4F$	5.1[c]	$Cu^{2+/3+}$	145	–	[16]
$LiCoOSO_4$	5.1[c]	$Co^{3+/4+}$	152	–	[16]
$LiNiOSO_4$	5.0[c]	$Ni^{3+/4+}$	152	–	[16]
Li_2NiSiO_4	4.8[c]	$Ni^{2+/3+}$	163[b]	–	[18]
$LiNi_{0.5}Mn_{1.5}O_4$	4.7	$Ni^{2+/3+/4+}$	147	3.5–4.9	[19]
$LiCr_yMn_{2-y}O_4$ ($0.5 \le y \le 1$)	~4.5–4.8	$Cr^{3+/4+}$, $Mn^{3+/4+}$	~151	3.4–5.4	[20,21]
$LiCo_yMn_{2-y}O_4$ ($0.5 \le y \le 1$)	~4.5–4.9	$Co^{3+/4+}$, $Mn^{3+/4+}$	~145	3.0–5.3	[22–24]
$LiFe_{0.5}Mn_{1.5}O_4$	4.5	$Fe^{3+/4+}$, $Mn^{3+/4+}$	148	3.0–5.3	[25,26]
$LiCu_{0.5}Mn_{1.5}O_4$	~4.3	$Cu^{2+/3+}$, $Mn^{3+/4+}$	145	3.3–5.1	[27–29]
$xLi_2MnO_3 \cdot (1-x)LiMeO_2$ ($0 < x < 1$, Me = Ni, Co, Mn)	3.5	$Ni^{2+/3+/4+}$, $Co^{3+/4+}$, $Mn^{3+/4+}$	~314[d]	2.0–4.8	[30]
$LiNiVO_4$	4.8	$Ni^{2+/3+}$	148	3.0–5.3	[31]

[a] $M^{x+/y+/z+}$ means three couples: $M^{x+/y+}$, $M^{y+/z+}$, and $M^{x+/z+}$.
[b] The capacities are based on the extraction of one Li^+ per formula.
[c] The data are obtained by theoretical estimation, and no experimental data are available.
[d] The capacity is based on the extraction of one Li^+ per formula, and the practical capacity may exceed the data.

are completely extracted up to 4.8 V, whereas only two Li ions are extracted between 3.0 and 4.3 V. Such materials face similar problems under high potentials.

2.1. Phosphates and fluorophosphates

$LiCoPO_4$ was firstly reported by Amine et al. [44] in 2000, which has received particular attention due to the high redox potential of 4.8 V vs. Li/Li^+ and thus high energy density of ~800 Wh kg^{-1}, making it the most promising candidate among olivine phosphates as the cathode material for high-voltage LIBs. However, its electrochemical performance is unsatisfactory due to the low electronic conductivity (3.4×10^{-9} S cm^{-1}) and low Li^+ ionic conductivity relating to the one-dimensional (1D) ion transport channel [45]. Also, the decomposition of electrolytes under high potentials results in poor cyclic stability (the electrolytes will be discussed in Section 3). Several strategies have been proposed to increase the conductivity, such as doping with metal ions, decreasing the particle size, and modifying the surface.

The metal ions could be doped on both Li sites (M1 sites) and Co sites (M2 sites). Although the mechanism is controversial, the electronic conductivity of $LiCoPO_4$ is increased after doping with aliovalent metal ions. Doping aliovalent metal ions on the M2 sites increases the lattice constant *c*, which enlarges the 1D channel and facilitates the Li^+ ion transport. Wang et al. [46] reported $Li_{1.025}Co_{0.95}V_{0.05}(PO_4)_{1.025}/C$ with an initial discharge capacity of 134.8 mAh g^{-1} at 0.1 C rate, and the capacity retention was 85% after 25 cycles. The divalent doping with Fe, Mn, and Ni could form olivine solid solutions, which demonstrate multiple charge/discharge plateaus [47,48]. The performance could be improved especially by doping with certain concentration of Fe [49]. However, the superiority of high-voltage plateaus would be weakened if the content of Fe is higher than 10% [50,51].

Although Li ion diffusion could be improved by doping to some degree, decreasing the particle size is a more direct and effective way. Several synthesis methods have been reported, such as lower-temperature synthesis using $NH_4CoPO_4 \cdot H_2O$ as the precursor [7,52], ball-milling with lower synthetic temperature [53,54], and heating under low oxygen partial pressure [45]. During these routes, carbon was generally employed to form composites with $LiCoPO_4$ to restrict the growth of the particles and improve the electronic conductivity [55–57]. Carbon simply mixed with $LiCoPO_4$ could not distribute homogeneously, and the surface encapsulation of conductive carbon layers has proved a better way [58–61]. Liu et al. [62] prepared carbon-coated $LiCoPO_4$ nanoporous microspheres with a diameter of ~70 nm by spray pyrolysis from precursor solutions (Fig. 1). $LiCoPO_4/C$ composites were tested in a lithium bis(oxalato)borate (LiBOB)-containing electrolyte, and exhibited a discharge capacity of 123 mAh g^{-1} at 0.1 C with a coulombic efficiency of 97% in the first cycle. The capacity retention was 95% after 20 charge/discharge cycles. Wang et al. [63] synthesized hedgehog-like $LiCoPO_4$ with hierarchical microstructures via a solvothermal method in the water/benzyl alcohol mixed solvent at 200 °C. The synthesized $LiCoPO_4$ was composed of nanorods with the diameter of ~40 nm and the length of ~1 μm, and a carbon shell of ~8 nm in thickness. The composite demonstrated an initial discharge capacity of 136 mAh g^{-1} at 0.1 C and retained 91% after 50 cycles. Surface modifications with other coating layers, such as $LiFePO_4$ [64], have also been reported to enhance the performance. Generally, surface coating on $LiCoPO_4$ is more difficult than that on other phosphates due to the surface properties [65]. The cyclic stability and rate performance of $LiCoPO_4$ are inferior compared with $LiFePO_4$ unless better modification methods are proposed. The lower temperature performance of $LiCoPO_4$ also needs to be improved, which is the common fault of phosphates.

Another candidate for high-voltage cathode materials in phosphates is monoclinic $Li_3V_2(PO_4)_3$ (LVP). $Li_3V_2(PO_4)_3$ has two crystal structures: rhombohedral NASICON-type structure and monoclinic structure [66]. The rhombic $Li_3V_2(PO_4)_3$ could only be synthesized by ion exchange of the corresponding sodium salt. The monoclinic $Li_3V_2(PO_4)_3$ was firstly reported by Saïdi et al. [67] in 2002 and has been extensively studied since then. Although the average discharge potential of $Li_3V_2(PO_4)_3$ is 3.8 V when charged to 4.8 V, the highest theoretical capacity (197 mAh g^{-1}) among phosphate cathodes assures high energy density (Fig. 2a). The 3D network structure allows rapid, isotropic ionic diffusion. However, the VO_6

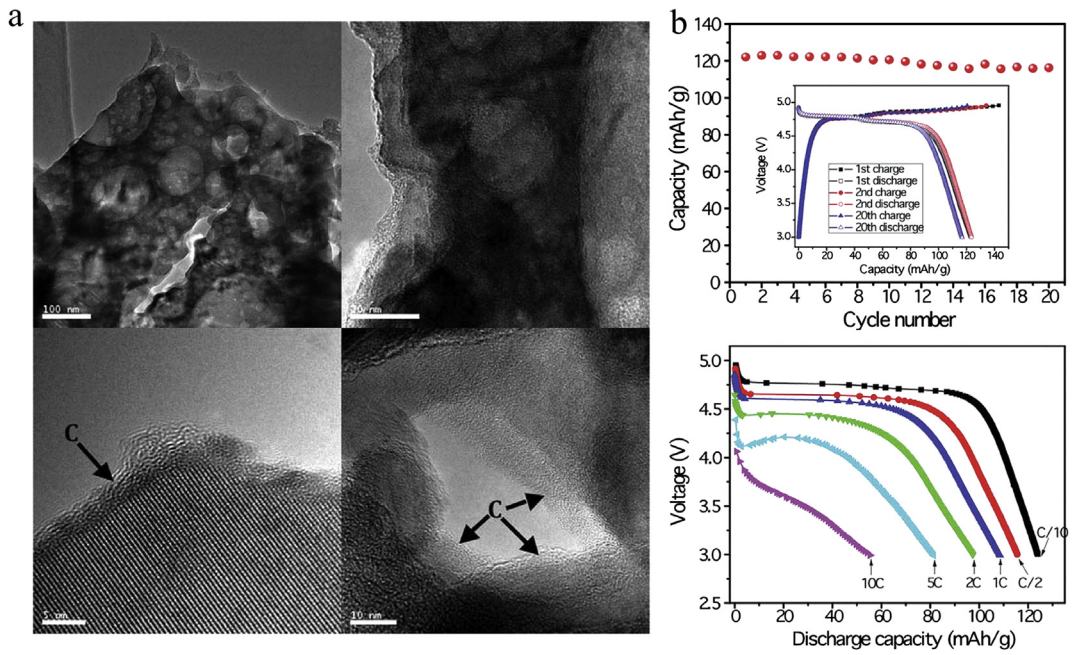

Fig. 1. Transition electron microscopy (TEM) images of nanoporous $LiCoPO_4/C$ composites (a); cyclic performances at 0.1 C (inset shows the charge/discharge curves at 0.1 C for various cycles) and discharge capacities at different rates (b). Taken from Ref. [62]. Copyright 2011, Royal Society of Chemistry.

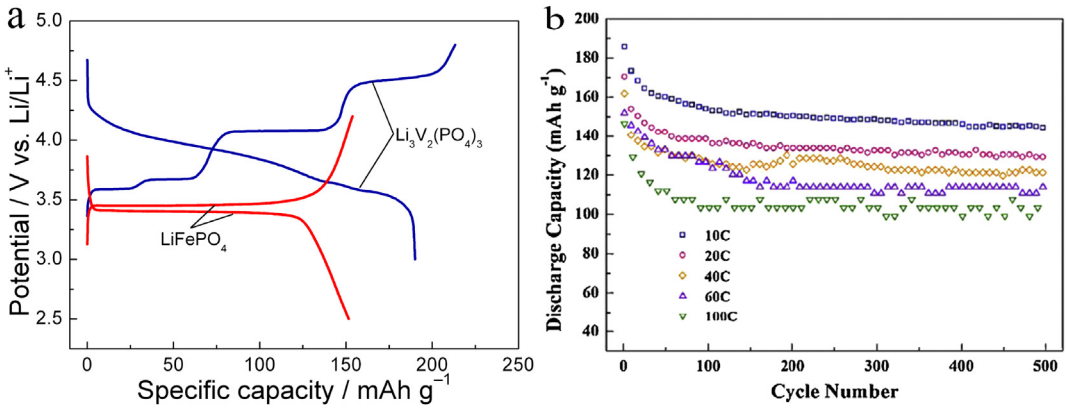

Fig. 2. Charge/discharge curves of $Li_3V_2(PO_4)_3$ compared with $LiFePO_4$ (a). Cyclic performance of $Li_3V_2(PO_4)_3$/C composites at the rates of 10–100 C between 3.0 and 4.8 V (b). Taken from Ref. [90]. Copyright 2012, Elsevier.

octahedrons are separated by the PO_4 tetrahedrons in the lattice, leading to low electronic conductivity. Substituting other metal ions for V and surface modifications with conductive materials are the main approaches to improve the performance. The doping ions could improve the structural stability as well as the electronic conductivity, which include Mg [68–70], Al [71,72], Sc [73,74], Ti [75], Cr [76,77], Mn [78], Fe [79], Co [80], Nb [81], and Ce [82]. Doping two different ions simultaneously [73,83] and doping halide ions [84] have also been proposed.

$Li_3V_2(PO_4)_3$ is usually synthesized by solid-state reactions. Although the solid carbon sources are always employed, the distribution of carbon on the bulk materials is not so uniform. The microparticles produced through high temperatures are also not beneficial for Li^+ diffusion. Compared with solid-state reactions, surface modifications with carbon through liquid-phase reactions provide more complete and homogeneous coating layers [85–87]. Sol–gel method is the most common choice [88,89]. Zhang et al. [90] synthesized porous $Li_3V_2(PO_4)_3$/C composites via a sol–gel-combustion method. The diameters of LVP particles and the pores were about 100–150 nm and 10–25 nm, respectively, with an amorphous carbon shell of ~4 nm in thickness. The $Li_3V_2(PO_4)_3$/C cathodes exhibited extremely high capacity and cyclic stability due to the special porous structure and the nanosized particles. The discharge capacities were 122, 114, 108 and 88 mAh g^{-1} at high rates of 10, 20, 40 and 60 C in the potential range of 3.0–4.3 V after 100 cycles, respectively. When cycled in the potential range of 3.0–4.8 V after 500 cycles, the discharge capacities were 145, 129, 122, 114 and 103 mAh g^{-1} at 10, 20, 40, 60 and 100 C, respectively (Fig. 2b). Graphene was also used to form composites with $Li_3V_2(PO_4)_3$ [91,92], which was widely explored in transition metal oxide anodes and could remarkably enhance the performance. However, the morphological control of $Li_3V_2(PO_4)_3$/graphene is more difficult due to the subsequent phase formation process under elevated temperatures for long time. The large particles could not be enwrapped entirely by graphene, and the rate performance still needs to be further improved by more effective morphological control method. Surface modifications with oxides and other compounds, such as MgO [93], SiO_2 [94], and $Li_4P_2O_7$ [95], could improve the structural stability of $Li_3V_2(PO_4)_3$. The oxide and phosphate coating layers could decrease the contact of the cathode surfaces with the electrolytes, and consume HF to inhibit the vanadium dissolution. However, the introduction of insulating layers may lead to the increase of interface charge transfer resistance, and the coexistence with carbon is necessary.

The general performance of $Li_3V_2(PO_4)_3$ between 3.0 and 4.3 V is comparable to commercial $LiFePO_4$. However, capacity fading occurs when it is cycled between 3.0 and 4.8 V due to the structural transition and the electrolyte decomposition on the electrode surface. Further studies should focus on these problems, as well as low temperature performances.

The fluorophosphates (Li_2MPO_4F, M = Co, Ni) allow high operating potentials due to the high electronegativity of fluorine and the strong ionicity of M–F bonds. Li_2CoPO_4F exhibits a high discharge plateau of ~4.9 V vs. Li/Li^+ with a theoretical capacity of 286 mAh g^{-1} if two Li^+ ions are extracted. However, only one Li^+ could be extracted below 5.5 V [39]. The crystal structure studied by precession electron diffraction (PED) discloses that the Li^+ ions are located at two sites, and the bond valence sum for the Li^+ ions at 8d sites is lower, indicating that the Li^+ ions are underbonded in the structure, which is responsible for the Li^+ extraction/insertion behavior in Li_2CoPO_4F; the bond valence sum for the Li^+ ions at 4c sites equals to the normal valence of +1, and they are difficult to be extracted [96]. Besides, the Li^+ ions are extracted by two steps in the first cycle, and then extracted by one step in the following cycles, indicating the structural transformation during the first cycle [13]. Khasanova et al. [97] supposed that the irreversible structural transformation could facilitate the Li^+ ion migration upon subsequent cycles. Li_2CoPO_4F has been synthesized by solid state reaction, spark plasma sintering, and sol–gel method [12,13,98,99]. The cyclic performance is unsatisfactory due to the low ionic and electronic conductivity, as well as the serious electrolyte decomposition on the cathode surface under high potentials. Similar to other phosphate cathode materials, nanosized particles and uniform carbon coating could reduce the ion diffusion length and enhance the electronic conductivity [12]. The application of electrolytes with high anodic stability also benefits the performance of Li_2CoPO_4F significantly [13]. Up to now, the knowledge about Li_2CoPO_4F is rather preliminary, and more extensive investigations are needed.

2.2. Spinel type high-voltage cathode materials

The spinel $LiMn_2O_4$ is a popular cathode material due to its low cost, environmental amity, and good safety. The MnO_2 framework provides 3D Li^+ diffusion pathways, and delivers high rate capability. However, $LiMn_2O_4$ suffers from serious problems of capacity fading, especially cycled at elevated temperatures. The reasons for the capacity decay include the irreversible structural transition from spinel to tetragonal structure caused by the Jahn–Teller distortion of Mn^{3+}, and the dissolution of Mn ions in the electrolytes by the corrosion of H^+. More importantly, the energy density of $LiMn_2O_4$ is not competitive with other cathode materials due to the common electrode potential (4.0 V vs. Li/Li^+) and the low theoretical capacity (148 mAh g^{-1}).

Fortunately, replacing Mn partly with other metal ions proves an effective strategy to improve the performances of $LiMn_2O_4$. The dopants suppress the Jahn–Teller distortion of Mn^{3+} and enhance the structural stability; therefore, the cyclic performance is improved accordingly. Among various doping derivatives, $LiNi_{0.5}Mn_{1.5}O_4$ is the most promising material combining good cyclic stability with high operating voltage. The valence of Ni in $LiNi_{0.5}Mn_{1.5}O_4$ is +2, and all the Mn ions are promoted to +4. The redox couples of $Ni^{2+/3+}$ and $Ni^{3+/4+}$ possess the approximate Fermi energy, exhibiting a rather flat discharge plateau around 4.7 V vs. Li/Li^+. Therefore, $LiNi_{0.5}Mn_{1.5}O_4$ displays both high energy density and power density.

$LiNi_{0.5}Mn_{1.5}O_4$ has two crystal structures: non-stoichiometric disordered $LiNi_{0.5}Mn_{1.5}O_{4-\delta}$ with $Fd\bar{3}m$ space group, and stoichiometric ordered $LiNi_{0.5}Mn_{1.5}O_4$ with $P4_332$ space group. In disordered $LiNi_{0.5}Mn_{1.5}O_{4-\delta}$, Ni and Mn ions are randomly occupied in 16d octahedral sites. The Li ions are occupied in tetrahedral 8a sites, and migrate via vacant octahedral 16c sites in the 8a–16c diffusion paths. In the ordered $LiNi_{0.5}Mn_{1.5}O_4$, Ni and Mn ions are occupied in 4a and 12d sites, respectively. However, the vacant octahedral 16c sites are split into ordered 4a and 12d sites. Li ions are located at 8c sites and transfer via the 8c–4a and 8c–12d diffusion paths [100]. Ordered Ni and Mn ions hinder the lithium ion diffusion [101] (Fig. 3). Besides, the small amount of Mn^{3+} ions in disordered $LiNi_{0.5}Mn_{1.5}O_{4-\delta}$ can increase the electronic conductivity. Therefore, disordered $LiNi_{0.5}Mn_{1.5}O_{4-\delta}$ exhibits better rate capability than ordered $LiNi_{0.5}Mn_{1.5}O_4$.

The synthesis of disordered $LiNi_{0.5}Mn_{1.5}O_{4-\delta}$ under high temperature is always accompanied by the generation of rock-salt $Li_xNi_{1-x}O$ impurities [102,103]. The Mn^{2+} ions produced from the disproportionation of the residual Mn^{3+} will also dissolve into the electrolytes, leading to the capacity loss, especially cycled at elevated temperatures. Slow cooling from the calcination temperature could effectively eliminate the rock-salt phase [104], and doping with other metal ions would decrease the Mn dissolution. Also, the metal dopants improve the electrochemical performances, by promoting the disorder distribution of Ni and Mn ions in the 16d sites, eliminating the $Li_xNi_{1-x}O$ impurities, improving the electronic conductivity and the Li^+ diffusion kinetics, and decreasing the undesired solid electrolyte interface (SEI) films by the enrichment of dopants and the deficiency of Ni ions on the surfaces. Wang et al. [105] reported that Ru-doped $LiNi_{0.5}Mn_{1.5}O_4$ delivered a capacity of 135 mAh g^{-1} and excellent cyclic performance at the 10 C charge/discharge rate for 500 cycles. The performance of $LiNi_{0.5}Mn_{1.5}O_4$ at elevated temperatures could be improved by replacing partial Ni ions with Cr ions [106–108]. Other metal dopants (such as Mg [109], Ti [103], Fe [110,111], Co [112], Zn [113], Cu [114], and Nb [115]) also have similar effects, and enhance the performance more or less. However, too many dopants enriched in the surfaces would increase the charge transfer resistance and degrade the rate performance [116]. The fluorine anion doping has been reported to improve the reversible capacity by the suppression of impurity phase and the variation in lattice parameter, as well as reduced Mn dissolution by the attack of HF [117,118].

The introduction of Ni ions to the spinels also causes the adverse effects. The electrolytes may decompose on the cathode surfaces due to the high potentials of $Ni^{2+/4+}$, and generate thick SEI films. Surface modifications of $LiNi_{0.5}Mn_{1.5}O_4$ with stable coating layers could inhibit the surface side reactions, as well as the Mn^{2+} dissolution into the electrolytes. Surface coating with oxides, such as ZnO [119–121], Al_2O_3 [34,122], BiOF [123], Bi_2O_3 [124,125], SiO_2 [126], ZrO_2 [127], and $La_{0.7}Sr_{0.3}MnO_3$ [128], and phosphates, such as Li_3PO_4 [129], $Li_4P_2O_7$ [130], $AlPO_4$ [131], $FePO_4$ [132], and $LiFePO_4$ [133], can enhance the cyclic stability and the performance at elevated temperatures. Metals, such as Ag [134] and Au [135], have also been adopted as coating layers. Ag was deposited on the surface of $LiNi_{0.5}Mn_{1.5}O_4$ and was changed into Ag_2O nanoclusters during the charge/discharge cycles, which improved the cyclic stability at low rates by reducing the reactivity of the spinels toward the electrolytes. However, Ag_2O formed an energy barrier and hindered Li^+ transfer between the electrode and electrolyte, degrading the rate capability [134]. The Au coating layers exhibited similar characters. As widely used coating layers, amorphous carbon [136] and conducting polymers [137] not only decreased the Mn^{2+} dissolution and avoided the formation of undesired thick SEI layers, but also improved the electronic conductivity of the cathode materials.

The morphology plays an important role of the performance of $LiNi_{0.5}Mn_{1.5}O_4$. Nanostructures may reduce Li^+ diffusion length, and improve the ionic conductivity. Shaju et al. [138] synthesized porous $LiNi_{0.5}Mn_{1.5}O_4$ nanoparticles by a resorcinol-formaldehyde assisted solution method, and the sample exhibited an initial capacity of 129 mAh g^{-1} at 10 C and 118 mAh g^{-1} at 20 C. However, the large surface area of the nanostructures might bring more side reactions with the electrolytes, resulting in low coulombic efficiency and severe capacity decay. Chen et al. [139] synthesized microsized

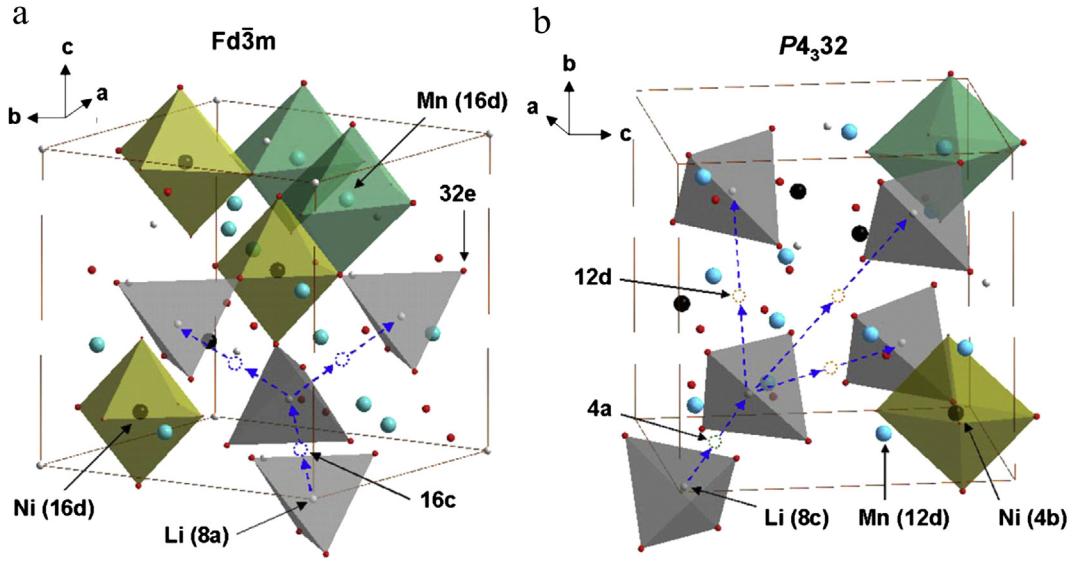

Fig. 3. Lithium ion diffusion paths in $LiMn_{1.5}Ni_{0.5}O_4$ spinels with the space group of $Fd\bar{3}m$ (a) and $P4_332$ (b). Taken from Ref. [101]. Copyright 2012, Elsevier.

$LiNi_{0.5}Mn_{1.5}O_4$ particles via an in situ template method, and the particles were fabricated by nanoflakes stacked orienting the (001) planes. The growth of the unstable (111) planes was inhibited in the surfaces, suppressing the Mn dissolution. The large interspaces between the nanoflake layers allowed fast Li^+ insertion/extraction. The synthesized $LiNi_{0.5}Mn_{1.5}O_4$ maintained 86% of the initial capacity (133.5 mAh g^{-1}) at 1 C after 500 cycles and exhibited a capacity of 96 mA h g^{-1} at 50 C.

The unique performance of $LiNi_{0.5}Mn_{1.5}O_4$ cathode materials promotes the investigations on full cells. The spinel $Li_4Ti_5O_{12}$ has been widely studied as a candidate for commercial anode materials due to its safety, excellent cyclic stability and rate performance [140–142]. The discharge plateau of ~1.5 V vs. Li/Li^+ avoid the side reactions with the electrolytes and the deposition of metallic Li [143,144]. However, the relatively higher potential of $Li_4Ti_5O_{12}$ compared with graphite requests much higher discharge potentials of the matched cathodes to deliver desirable energy densities. The 3 V $LiNi_{0.5}Mn_{1.5}O_4/Li_4Ti_5O_{12}$ cells have been reported by Jung et al. [145], which exhibited a capacity of 107 mAh g^{-1} at a high rate of 10 C, and retained 85.4% of its initial capacity after 500 cycles at 1 C rate. The cells delivered a very stable capacity in the temperature range from −20 to 55 °C. The energy density reached 372 Wh kg^{-1}, which is considerably higher than that of the presently available commercial LIBs. Other titanium oxide-based anodes, such as TiO_2 [146] and $TiNb_2O_7$ [147], were also combined with $LiNi_{0.5}Mn_{1.5}O_4$ and displayed good cyclic performance. The adoption of low potential anodes, like mesocarbon microbead (MCMB) [148], Si [149], and Sn [150], could deliver higher operating voltages. Hassoun et al. [151] reported that the $Li[Ni_{0.45}Co_{0.1}Mn_{1.45}]O_4$/Sn–C cells offered excellent cyclic stability at 1 C rate after 90 cycles, and still kept 108 mAh g^{-1} at 5 C (Fig. 4). The calculated energy density was as high as 500 Wh kg^{-1}. Besides, $LiNi_{0.5}Mn_{1.5}O_4$/Sn–C Li ion polymer batteries were thermally stable at the temperatures up to ~200 °C without thermal decomposition, demonstrating high safety [152].

The $LiNi_{0.5}Mn_{1.5}O_4$ cathode material is very promising for high-voltage LIBs due to the high energy density and excellent electrochemical performance after modifications. The full cells with $LiNi_{0.5}Mn_{1.5}O_4$ as cathode materials exhibit great commercial prospects. However, the performance at elevated temperatures is unsatisfactory resulting from the Mn dissolution and the side reactions with the electrolytes. Doping and surface modifications have proved effective methods to solve the problem. In addition, the conventional electrolytes are unstable at high potentials, which need to be optimized for high-voltage LIBs.

2.3. Li-rich layered oxide cathode materials

The layered transition metal oxides with α-$NaFeO_2$ crystal structure are the most common cathode materials for LIBs.

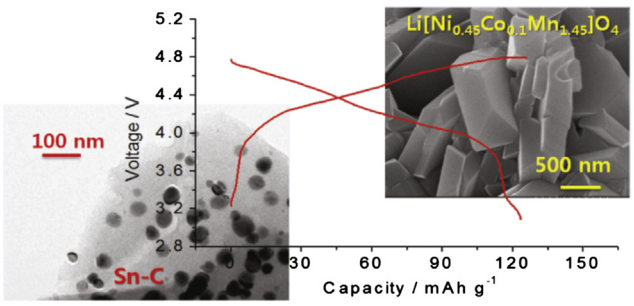

Fig. 4. The morphologies of the $Li[Ni_{0.45}Co_{0.1}Mn_{1.45}]O_4$ cathodes and the Sn–C anodes, and the charge/discharge curves of the $Li[Ni_{0.45}Co_{0.1}Mn_{1.45}]O_4$/Sn–C cells. Taken from Ref. [151]. Copyright 2011, American Chemical Society.

Although $LiCoO_2$ has been widely used in portable electronic devices, the high cost of Co and safety issues inhibit the application in EVs and HEVs. Replacing certain amount of Co with resource-abundant Ni and Mn (represented by $LiMeO_2$, Me = Ni, Co, and Mn) may decrease the cost and the structural instability [153]. However, the energy density is not significantly improved compared with $LiCoO_2$. Recent investigations on layered oxide cathodes mainly focus on the combination of $LiMeO_2$ with layered Li_2MnO_3. The $xLi_2MnO_3\cdot(1-x)LiMeO_2$ solid solution exhibits an extreme high discharge capacity of over 300 mAh g^{-1} when cycled between 2.0 and 4.8 V. The average discharge potential is rather low; however, the high capacity derives from the charge plateau above 4.5 V; therefore, the Li-rich layered oxides are also expounded in this section.

The structure of $xLi_2MnO_3\cdot(1-x)LiMeO_2$ is similar to $LiMeO_2$, and the only difference is that the excessive Li^+ ions substitute for part of the transition metal ions and occupy the MO_6 octahedra sites. However, it is still under debate whether $xLi_2MnO_3\cdot(1-x)LiMeO_2$ is a homogeneous solid solution which is not separated into $LiMeO_2$ and Li_2MnO_3 regions [154], or a composite constituted by $LiMeO_2$ and Li_2MnO_3 [155,156]. Nevertheless, the structure appears homogeneous over long range. The origin of the unique high discharge capacity that exceeds the theoretical value (extra capacity) and the charge/discharge processes are unclear. The charging stage below 4.5 V corresponds to the oxidization of Ni^{2+} and Co^{3+} to Ni^{4+} and Co^{4+}, respectively. The valence of Mn which is already +4 keeps unchanged, and the structural distortion around the Mn ions was observed by Mn K-edge XANES (X-ray absorption near edge structure) [157]. When charging across the plateau at 4.5 V, part of the metal ions are reduced accompanied with the removal of Li and O. The Mn ions are activated due to the reduction and will participate in the following electrochemical reactions. The removal of Li and O from the lattice leads to the structural rearrangement, and the metal ions may migrate to the Li layers [158–160]. Then a defect spinel phase generates on the surface, which has been confirmed by HAADF STEM (high angle annular dark field scanning transmission electron microscopy) techniques [161,162] (Fig. 5). Part of the removed oxygen forms oxygen molecules, which may be reduced in the discharge stage and provide extra capacity. Although some oxygen vacancies remain on the surface after the discharge process, the majority of oxygen vacancies are eliminated, as well as certain amount of cation sites (including the sites in transition metal layers and lithium layers), resulting in large irreversible capacity.

The large irreversible capacity is adverse to the design of full cells and battery packs accordingly. Several methods have been proposed to reduce the irreversible capacity. The treatment with HNO_3 could increase the coulombic efficiency to nearly 100% by leaching Li_2O from the lattice [163,164]. However, the acid treatment damaged the cyclic stability due to the Li^+/H^+ exchange. The further treatment with NH_3 at 200 °C could eliminate the shortcoming [165]. The treatment with $Na_2S_2O_8$ [166] and $(NH_4)_2SO_4$ [167] could also extract lithium and oxygen, and the spinel phase formed on the surface, which decreased the charge transfer resistance and facilitated the lithium ion diffusion. The composites of Li-rich oxides and lithium insertion hosts, such as V_2O_5, $Li_4Mn_5O_{12}$, and LiV_3O_8, exhibited high coulombic efficiency of 100% [168,169]. The extracted Li^+ ions in the charge process could insert into the host, and then be extracted in the discharge process, attributing to extra discharge capacity. Partially substituting Ru for Mn also increased the coulombic efficiency [170]. The treatment with mildly acidic fluorinated solutions (such as NH_4PF_6, $(NH_4)_3AlF_6$, and NH_4BF_4) passivated the surface by forming a stable fluorinated layer, which decreased the impedance and enhanced the discharge capacity [171]. The surface modifications with other coating layers

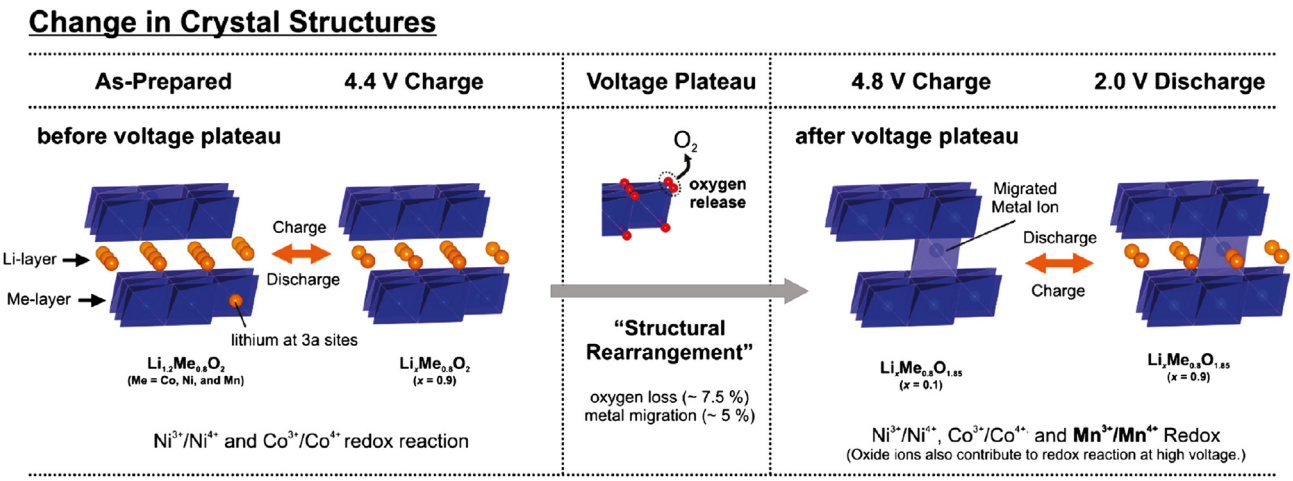

Fig. 5. Schemes of the crystal structural change mechanisms of $Li_{1.2}Ni_{0.13}Co_{0.13}Mn_{0.54}O_2$ charged/discharged between 2.0 and 4.8 V. Taken from Ref. [158]. Copyright 2011, American Chemical Society.

also improved the coulombic efficiency to some degree. Besides, the coating layers effectively improved the cyclic stability and rate performance. The performance improvement is attributed to different mechanisms, such as the inhibition of the electrolyte decomposition [172–176], the decrease of charge transfer resistance [177–180], the facilitation to lithium ion diffusion [179–183], the scavenging of HF [184,185], the retaining of more oxide ion vacancies [176,186–188], the transformation of the surface to spinel phase [189], and the suppression of ion rearrangements as well as the micro strain on the surface by enhancing the structural stability [187]. Replacing Mn with other metal ions also influenced the performance. The Cr dopants could act as a catalyst for the activation of Li_2MnO_3 component [190]. Deng et al. [191] reported that substituting Co for Mn increased the oxygen loss and the charge/discharge capacity consequently, while the substitution of Ti for Mn played the opposite role. The phenomenon was due to the covalence of the metal–oxygen bonds associating with the overlap degree of the metal ions with the O_{2p} orbital. Substituting sulfur for oxygen improved the cyclic performance of the materials by improving the structural stability [192].

In summary, Li-rich layered oxides demonstrate high energy densities when operated under high potentials. The complex structural transition leads to low coulombic efficiency. The structural instability and surface reactions with electrolytes result in serious capacity decay. Surface modifications are the main approaches to improve the performance of Li-rich layered oxides. However, the poor rate performance caused by low electronic conductivity and Li^+ diffusion kinetics are the limitations of this material.

3. High-voltage electrolytes

Electrolytes are the indispensable part of LIBs, which directly affect the electrochemical behavior through the interface reactions with the electrodes and its Li^+ ion diffusion characters. The electrochemical windows of the electrolytes represent the energy separation of the lowest unoccupied molecular orbital (LUMO) and the highest occupied molecular orbital (HOMO). The cathodes with the potentials below the HOMO of electrolytes will cause the electron transfer from the electrolytes to the cathodes, and lead to the oxidation of the electrolytes. The requirement of high-voltage cathode materials is a great challenge for the conventional electrolytes, which trend to be oxidized at ~4.5 V [193]. Although the oxidization potentials of organic carbonate solvents are about 5 V, the transition-metal ions could catalyze the oxidation reaction and accelerate the decomposition of electrolytes at lower potentials, leading to rapid capacity fading [194]. Therefore, searching for matched electrolytes is essential to the realization of high-voltage LIBs. The present studies on high-voltage electrolytes mainly focus on novel stable solvents and functional additives.

3.1. Solvents

Compared with organic carbonate solvents, room temperature ionic liquids (RTILs) exhibit high thermal stability, low flammability, low volatility, and wide electrochemical windows [195]. The high electrochemical stability makes RTILs candidate electrolytes for high-voltage LIBs. The electrochemical windows are determined by the electrochemical stability of the anions and cations themselves, and the anodic and cathodic stability are limited by the anions and cations, respectively. Meanwhile, the interactions of the anions and cations might also exist and affect the anodic and cathodic stability [196]. The anodic stability of imidazolium salts is appropriate. However, the reduction potentials are located at ~1.5 V vs. Li/Li^+ [197,198], and the cations will decompose on the anodes. The piperidinium and pyrrolidinium salts exhibit lower reduction potential and higher oxidization potentials of ~6 V vs. Li/Li^+ [197], which are promising electrolyte solvents for high-voltage LIBs. Borgel et al. [199] studied the performance of $LiNi_{0.5}Mn_{1.5}O_4$/Li cells in the N-methyl-N-propylpiperidinium bis(trifluoromethanesulfonyl) imide ($PP_{13}TFSI$) electrolyte containing 0.4 M LiTFSI at 1/16 C. The initial coulombic efficiency was much higher than that of the cells cycled in the ethylene carbonate (EC)/ethyl methyl carbonate (EMC) electrolyte containing 1.5 M $LiPF_6$, indicating that the side reactions were inhibited due to the high anodic stability of the electrolyte. It has also been reported that the surface films forming in the N-methyl-N-propylpyrrolidinium bis(trifluoromethylsulfonyl) imide (PMPyrTFSI)/LiTFSI electrolyte passivated the $LiNi_{0.5}Mn_{1.5}O_4$ electrodes and improved the performance at elevated temperatures [200]. However, the disadvantages of high viscosity and low ionic conductivity of RTILs result in poor cyclic stability and rate capability. The compatibility with the electrodes is also unsatisfactory due to the low wettability, and the high melting point degrades its low-temperature performance. The problems could largely be overcome by mixing RTILs with certain amount of conventional carbonate solvents [201] and other co-solvents [202], which do not have a pernicious influence on the anodic stability of RTILs [203]. Xiang et al. [204] reported that the rate capability and low-temperature

performance of the $LiCoO_2$/Li cells were improved by adding 20 wt.% diethyl carbonate (DEC) as a co-solvent into pure $PP_{13}TFSI$ based electrolyte. The introduction of ester additives (such as vinylene carbonate (VC), and ethylene sulfite (ES)) could suppress the reduction of RTILs and form stable SEI films on the anodes, enhancing the performance of the electrodes accordingly [205,206].

Sulfones have also been investigated as the electrolyte solvents of high-voltage LIBs due to their high anodic stability. The oxidization potentials of sulfones are around 5.5 V according to experimental and theoretical studies [207–209]. The functionalization with strong electron-withdrawing groups could further increase the oxidation potentials [210]. The viscosity of sulfones is lower than that of RTILs, which may exhibit better infiltration and compatibility with the electrodes. Stable SEI films could not form on graphite anodes by sulfones [211]. The introduction of additives such as VC [212,213], lithium difluoro(oxalate)borate (LiDFOB) [214], p-toluenesulfonyl isocyanate (PTSI) [215], hexamethylene diisocyanate (HDI) [216], and fluorination of the alkyl groups in sulfones [207] could overcome this shortcoming. In addition, the co-solvents are also introduced to decrease the viscosity and melting point, and improve both the conductivity and wettability [217–220]. Molecular dynamics (MD) simulations showed that the oxygen atoms of dimethyl carbonate (DMC) in tetramethyl sulfone (TMS)/DMC/$LiPF_6$ electrolyte did not approach the surface of the cathodes as close as in EC/DMC/$LiPF_6$ electrolyte; consequently, DMC molecules in TMS/DMC/$LiPF_6$ electrolyte are less likely to be oxidized than in EC/DMC/$LiPF_6$ electrolyte, which would not noticeably decrease the oxidative stability of sulfone-based electrolytes [221]. The performance of $LiNi_{0.5}Mn_{1.5}O_4/Li_4Ti_5O_{12}$ cells in the TMS/EMC (50:50 v/v) mixed electrolyte was reported by Abouimrane et al. [218], which delivered an initial capacity of 80 mAh g^{-1} and were cycled stably without significant capacity fading for 1000 cycles at 2 C rate. Although the performance is enhanced by the co-solvents, the rate performance of sulfone-based electrolytes is still inferior to the conventional electrolytes due to the higher viscosity [222].

Aliphatic dinitrile solvents like glutaronitrile could sustain up to ~8 V vs. Li/Li^+ [223,224], which is stable than most of the aprotic solvents. The co-solvents are required due to the easy reduction and poor compatibility of dinitriles with lithium or graphite anodes. Adding EC forms stable SEI films on the anodes, allowing reversible Li^+ extraction/insertion [225,226]. The EC/DMC/sebaconitrile (25:25:50 v/v) electrolyte containing 1 M $LiBF_4$ exhibited high electrochemical stability at 6.0 V on a $LiFePO_4$ electrode. Furthermore, the Li_2NiPO_4F cathode with a high redox potential located around 5.3 V vs. Li/Li^+ could be cycled reversibly in the sebaconitrile-based electrolyte [14]. The butyronitrile was also investigated as a co-solvent to the EC/EMC electrolyte to improve the high-temperature performance of $LiNi_{0.5}Mn_{1.5}O_4$/MCMB cells [227].

The fluorinated carbonate solvents, which have been employed as additives to help forming stable SEI films on the anodes [98,228,229], exhibit improved oxidation stability due to the high electronegativity and low polarity of fluorine atoms [230]. The redox potential of fluoroethylene carbonate (FEC) was higher than that of propylene carbonate (PC) on both platinum electrodes and activated carbon electrodes [231]. Sharabi et al. [232] reported that the cyclic performance of the $LiCoPO_4$ cathode was remarkably enhanced in the FEC/DMC electrolyte with 1 M $LiPF_6$ compared with that in the EC/DMC electrolyte containing 1 M $LiPF_6$ due to the formation of the protective interphase film on the cathode surfaces. Meanwhile, the lower ratio of electrolyte solution to the cathode resulted in better performance due to the decrease of the attack of F^- anions on the cathode material (Fig. 6). For the conventional $LiCoO_2$ cathode, the energy density could also be improved with higher cutoff voltage. However, the cutoff voltage is limited to ~4.3 V due to the structural collapse of the highly delithiated phase and the electrolyte decomposition [233]. Kitagawa et al. [234] reported that stable cyclic stability of $LiCoO_2$ with a high upper cutoff voltage of 4.5 V was observed in the FEC/1,1,2,2-tetrafluoro-3-(1,1,2,2-tetrafluoroethoxy) propane (1:1 v/v) electrolyte containing 1 M $LiPF_6$. The FEC based electrolyte formed a favorable interphase film on the $LiCoO_2$ cathode surface, and inhibited the further oxidative decomposition of the electrolyte at high potentials.

Although RTILs, sulfones, and nitriles exhibit high oxidization stability, the general problems of high viscosity, low conductivity, and low compatibility with the electrodes lead to poor performance compared with conventional electrolytes. The performance may be enhanced by adding co-solvents and additives. However, the rate performance is still unsatisfactory. The fluorinated carbonate solvents seem more appropriate for high-voltage LIBs in the current stage.

3.2. Additives

The SEI films could form on the anodes by the reduction of electrolytes or electrolyte additives, which protect the electrolytes from further decomposition. Although the formation mechanism is rather complicated and not definite, the importance of stable SEI

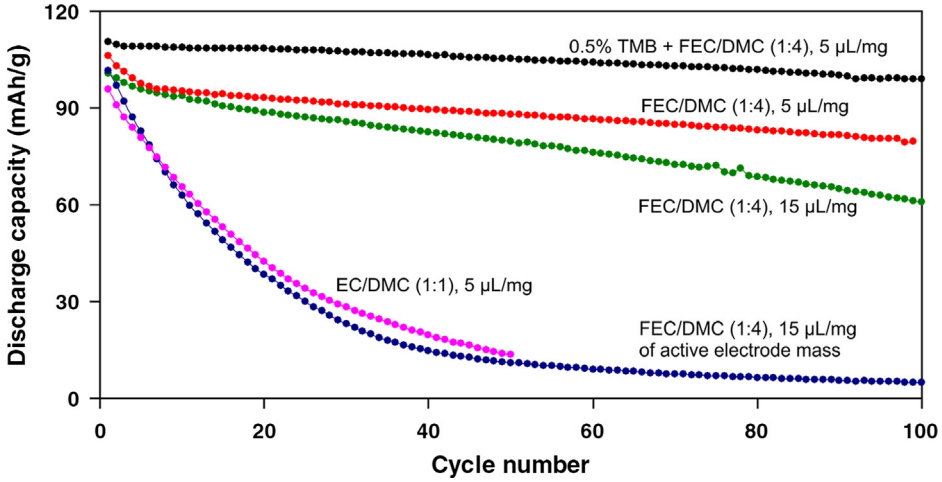

Fig. 6. Cyclic performance of $LiCoPO_4$/Li cells between 3.5 and 5.2 V in different electrolytes and with different amounts of electrolytes. TMB represents to trimethyl boroxine. Taken from Ref. [232]. Copyright 2013, Elsevier.

films on the anodes has been generally accepted [235–237]. Analogously, the oxidization of electrolytes under high electrode potentials also forms interphase films on the cathodes [238]. The films generated by the carbonate electrolytes are not uniform, and the electrolytes may decompose continuously, leading to high interphase resistance and capacity fading. To build stable interphase films on cathode surfaces, several electrolyte additives have been proposed, which have higher HOMO energy compared with the carbonate solvents and could be oxidized preferentially and isolate the electrolytes from the cathode surfaces. Then the decomposition of the electrolytes catalyzed by the transition metal ions can be inhibited accordingly. The additives that assist in forming cathode films include inorganic compounds and organic molecules.

LiBOB is a typical inorganic additive for high-voltage LIBs [239,240]. The oxidation of LiBOB on the cathode surface generates a cathode passivation layer, which inhibits further oxidation of the electrolyte. The cells containing LiBOB had lower impedance due to the thinner surface films [241]. Stable SEI films on anodes could also form by the reduction of oxalate in LiBOB [242,243]. Furthermore, LiBOB could act as Li salt to replace $LiPF_6$, inhibiting the generation of trace HF and the dissolution of metal ions on the cathode surfaces by the corrosion of HF consequently [148]. Compared with LiBOB, the interphase films formed by LiDFOB are more stable and exhibit lower interfacial resistance due to the lower content of easily oxidized or reduced oxalates, which benefit for the cyclic performance [244,245]. Hu et al. [246] reported that the cyclic stability of high-voltage $LiCoPO_4$ electrode was remarkably enhanced by the addition of LiDFOB to the electrolyte. The presence of B on the cathode surfaces was confirmed by X-ray photoelectron spectroscopy (XPS), indicating that LiDFOB participated in the formation of stable interphase films. Analogously, tetramethoxytitanium (TMTi) modified the structures of the cathode surface films, and the formation of PEC from EC was reduced, certified by the FTIR-ATR (Fourier Transform Infrared-Attenuated Total Reflectance) spectra [247] (Fig. 7). The cyclic performance was improved accordingly.

The organic additives include phosphides, sulfonate esters, monomers that can be electrochemically polymerized, carboxyl anhydrides, fluorine-containing compounds, as well as some special ethers and carbonates. The electrolytes containing certain ethers and carbonates, such as 2,5-dihydrofuran and γ-butyrolactone, showed higher anodic stability. Cyclic voltammetry (CV) tests on the glassy carbon electrodes showed that the oxidation current of the electrolytes decreased obviously after the first cycle due to the sacrificial oxidization of the additives on the electrodes and the formation of passivation layers preventing further oxidation of the electrolytes [248]. Phosphides (such as tris(pentafluorophenyl) phosphine (TPFPP), tris(hexafluoro-iso-propyl) phosphate (HFiP) and N-(triphenylphosphoranylidene) aniline (TPPA)), sulfonate esters (such as methylene methanedisulfonate (MMDS)), carboxyl anhydrides (such as glutaric anhydride and succinic anhydride), and fluorides (such as 1,1-difluoro-4-phenylbut-1-ene (DF)) exhibited similar surface-film-forming characters and enhanced the performance of high-voltage cathodes [249–255]. In addition, HFiP, DF, succinic anhydride, and 1,3-propane sultone formed stable SEI films on the anodes, which also benefit the performance of high-voltage LIBs [250,255,256]. It has been reported that tri-isopropoxy boroxine could act as anion receptors to stabilize the lithium salt LiTFSI, and the anodic stability of the electrolytes containing tri-isopropoxy boroxine was improved up to 5.0 V vs. Li/Li^+ on the $LiMn_2O_4$ film electrodes [257]. Trimethyl boroxine also improved the performance of $LiCoPO_4$ obviously [232]. The conventional additives, such as VC, could be polymerized at high potentials and protect the cathode surfaces [258,259]. However, the anodic stability of VC is insufficient, which may degrade the high-temperature cyclic stability under high electrode potentials due to its complete decomposition [256,260].

Molecular orbital calculations illustrate that benzene derivatives (such as biphenyl and o-terphenyl) and heterocyclic compounds (such as furan, thiophene, N-methyl pyrrole, and 3,4-ethylenedioxy thiophene (EDOT)) possess higher HOMO energy compared with carbonate solvents [261], which were consistent with the experimental results [262]. These additives are oxidized and electrochemically polymerized on the cathode surfaces prior to the electrolyte solvents. Particularly, the generated polymers possess conjugated π networks and demonstrate excellent electrical conductivity. Therefore, the

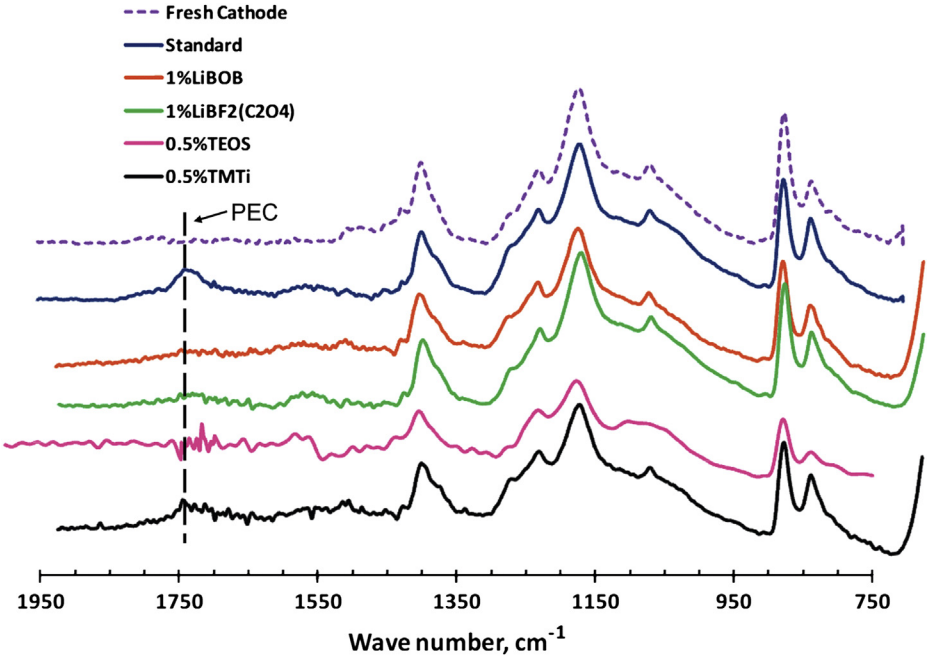

Fig. 7. FTIR-ATR spectra of the fresh and cycled $Li_{1.17}Mn_{0.58}Ni_{0.25}O_2$ electrodes between 2.0 and 4.9 V in the electrolytes with and without additives. Taken from Ref. [247]. Copyright 2011, Elsevier.

surface films formed by these additives not only suppress the decomposition of electrolytes, but also improve the electrical conductivity of the cathodes. Hu et al. [263] reported that thiophene was in situ electrochemically polymerized into polythiophene films, which coated uniformly on the $Li_3V_2(PO_4)_3$ cathode surfaces with the thickness of ~5–8 nm (Fig. 8), and decreased the catalytic decomposition of the electrolytes. Furthermore, the polythiophene films improved the electrical conductivity of $Li_3V_2(PO_4)_3$ and decreased the ohmic polarization, allowing higher reversible charge/discharge capacity and better rate performance. The polythiophene film, poly (3,4-ethylenedioxy thiophene) (PEDOT), and poly (3-hexyl thiophene) also improved the performance of $LiCoPO_4$ [264], $LiCoO_2$ (3–4.5 V) [265], $LiNi_{1/3}Co_{1/3}Mn_{1/3}O_2$ (3–4.6 V) [266], $Li_{1.2}Ni_{0.15}Co_{0.1}Mn_{0.55}O_2$ (3–4.9 V), and $LiNi_{0.5}Mn_{1.5}O_4$ [267], as well as the performance at elevated temperatures and thermal stability of the cells.

In summary, the additives for high-voltage LIBs are mainly based on the mechanism of assisting in forming stable interfacial films on the cathodes, which decrease the decomposition of the electrolytes under high potentials. The conducting polymers formed by the oxidization of the additives further improve the electronic conductivity of the cathode materials and enhance the performance.

4. Optimizations of other components in high-voltage LIBs

For the purpose of building advanced high-voltage LIBs, every component of the cells should be considered to match the high voltage. As conductive carbon additives, the high-surface-area carbon materials, such as Ketjen black and graphene, are generally considered better than the low-surface-area acetylene black and Super P due to the higher electronic conductivity. However, the surface functional groups of the high surface area carbon materials are oxidized at high potentials, and thick passivation films form on the cathode surfaces, resulting in low Coulombic efficiency and fast capacity decay [268]. The water-soluble binder carboxymethyl cellulose (CMC) was investigated to make $Li[Li_{0.2}Mn_{0.56}Ni_{0.16}Co_{0.08}]O_2$ electrodes for high-voltage LIBs instead of poly(vinylidene fluoride) (PVDF). The CMC-based electrodes showed improved cyclic stability and rate capability [269]. Xu et al. [270] reported that $LiNi_{1/3}Mn_{1/3}Co_{1/3}O_2$ electrodes with CMC binder cycled between 2.5 and 4.6 V exhibited similar results, due to the smaller charge transfer resistance and lower apparent activation energy of the CMC-based electrodes compared with the electrodes with PVDF binder.

Also, the appropriate anodic stability of separators and current collectors is essential due to the direct contact with the high-voltage cathodes [271]. The polyethylene (PE)-based separators were more stable than the polypropylene (PP)-based separators under high potentials due to the lower HOMO energy of PE, and the $LiCr_{0.05}Ni_{0.45}Mn_{1.5}O_4$/Li cells with PE-based separators showed enhanced cyclic stability and rate performance. In addition, Sharabi et al. [272] reported that the SiO_2-containing quartz separators significantly improved the capacity retention of $LiCoPO_4$ cathodes, which acted as an HF scavenger to prevent the detrimental reactions of the cathodes with the electrolytes. The separator containing lithiated $Li_4Ti_5O_{12}$ could scavenge the decomposition products of the electrolytes and the dissolved transition metal ions, which prevented the migration of decomposition products to the anode and side reactions [273]. Al is the most common cathode current collector. Although it is not confirmed that Al is stable enough above 5 V, Al current collector could be used in 5 V cells in the current stage due to the formation of dense alumina protective layer on the surface unless more appropriate current collectors are available. In addition, the surface treatment of Al current collectors (such as surface oxidation and fluorination) will enhance the oxidation stability and inhibit the corrosion. Chen et al. [274] reported that the Al-clad stainless steel positive cans exhibited better electrochemical stability than the bare stainless steel positive cans in the $LiCr_{0.05}Ni_{0.45}Mn_{1.5}O_4$/Li cells due to the generation of dense alumina protective layers on the surfaces. The reactions among the cathodes, the electrolytes, and the separators at high potentials might lead to undesired deposits on the separator surfaces, which degraded the performance of high-voltage LIBs.

The storage of high-voltage LIBs is another important issue. The $LiNi_{0.5}Mn_{1.5}O_4$/Li cells that were stored below 4.5 V showed low residual current. However, when stored at high voltages (4.7–5.3 V), the residual current increased rapidly, and the electrolyte decomposition product poly(ethylenecarbonate) with high content was observed [238,275]. Although the VC additive benefits the performance of high-voltage LIBs, the high content of unstable VC is detrimental to the storage at elevated temperatures under high potentials [260].

The safety features of high-voltage LIBs are critical, such as thermal stability, and overcharge protection. The dimethylmethyl phosphonate (DMMP)-based electrolyte exhibited high thermal stability and good compatibility with the $LiNi_{0.5}Mn_{1.5}O_4/Li_4Ti_5O_{12}$ cells [276]. The redox shuttle additive tetraethyl-2,5-di-tert-butyl-1,4-phenylene diphosphate (TEDBPDP) provided overcharge protection at 4.75 V vs. Li/Li^+ [277], and 1,2,3,4-tetrabromo-5,6-dimethoxy benzene exhibited higher redox shuttle potentials at ~5.05 V. However, the potentials are not high enough for 5 V cathode materials because the oxidation potential of the additives

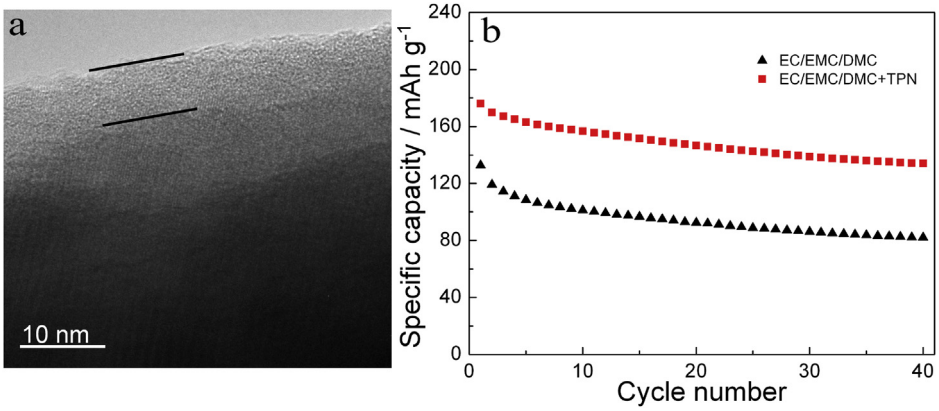

Fig. 8. High-resolution TEM image of the cycled $Li_3V_2(PO_4)_3$ cathodes in the electrolyte with thiophene (a); cyclic performance of $Li_3V_2(PO_4)_3$ cathodes in the electrolytes with and without thiophene (TPN) at 0.1 C (b). Taken from Ref. [263]. Copyright 2013, Elsevier.

had better be 0.3–0.4 V higher than the charge cutoff potentials [278], and new additives need to be developed.

In summary, the components except electrode active materials and electrolytes should also be considered carefully in high-voltage LIBs, even though they operate well in conventional LIBs. The optimization work is complicated, however, essential.

5. Conclusions and prospects

In this review we discussed the recent progress in high-voltage LIBs, including the promising high-voltage cathode materials, the matched electrolyte solvents, the electrolyte additives, and the optimizations of other cell components. Compared with the conventional cathode materials, the cyclic stability and rate performance of high-voltage cathode materials still need to be improved. Dopants enhance the intrinsic charge transfer and lithium ion diffusion kinetics, surface modifications improve the surface characters of the materials and inhibit the side reactions with the electrolytes, and the control of particle size is also an effective method to improve the performance. Meanwhile, considering the practical application of high-voltage LIBs, the control of particle size should be compromised with the volumetric energy density. The development of matched electrolyte systems is equally essential. The completely new electrolyte solvents with high anodic stability still encounter serious capacity fading and poor rate performance due to the high viscosity, poor wettability and SEI forming characters. Mixing with certain amount of carbonic esters could ameliorate the limitations. The high-voltage electrolyte additives are based on the principle of building stable interphase films on cathode surfaces, which inhibit the catalytic decomposition of the electrolytes by the transition metal ions. In addition, the interphase films forming through the electropolymerization of specific additives could improve the electrical conductivity of the cathode materials. The other components of the cells should also be considered to match the high-voltage cathodes. The combination of high-voltage cathode materials and stable anodes, as well as matched high-voltage electrolytes containing additives and other optimized components would certainly build advanced high-voltage LIBs with high energy and power density, which will drive the present LIBs to more fields. Significant progress has been made; however, great efforts are still needed.

Acknowledgments

This work was supported by the 973 Program (2009CB220100) and the Fundamental Research Funds for the Central Universities in China. The authors thank Dr. Dihua Wu for his help with the preparation of the graphical abstract.

References

[1] M. Armand, J.M. Tarascon, Nature 451 (2008) 652–657.
[2] J.B. Goodenough, Y. Kim, Chem. Mater. 22 (2010) 587–603.
[3] L. Su, Y. Jing, Z. Zhou, Nanoscale 3 (2011) 3967–3983.
[4] R. Marom, S.F. Amalraj, N. Leifer, D. Jacob, D. Aurbach, J. Mater. Chem. 21 (2011) 9938–9954.
[5] B. Xu, D. Qian, Z. Wang, Y.S. Meng, Mater. Sci. Eng. R 73 (2012) 51–65.
[6] A. Kraytsberg, Y. Ein-Eli, Adv. Energy Mater. 2 (2012) 922–939.
[7] J.M. Lloris, C. Pérez Vicente, J.L. Tirado, Electrochem. Solid-State Lett. 5 (2002) A234–A237.
[8] F. Zhou, M. Cococcioni, K. Kang, G. Ceder, Electrochem. Commun. 6 (2004) 1144–1148.
[9] H. Huang, S.C. Yin, T. Kerr, N. Taylor, L.F. Nazar, Adv. Mater. 14 (2002) 1525–1528.
[10] H. Kim, S. Lee, Y.-U. Park, H. Kim, J. Kim, S. Jeon, K. Kang, Chem. Mater. 23 (2011) 3930–3937.
[11] M. Tamaru, P. Barpanda, Y. Yamada, S.-I. Nishimura, A. Yamada, J. Mater. Chem. 22 (2012) 24526–24529.
[12] X. Wu, Z. Gong, S. Tan, Y. Yang, J. Power Sources 220 (2012) 122–129.
[13] D. Wang, J. Xiao, W. Xu, Z. Nie, C. Wang, G. Graff, J.-G. Zhang, J. Power Sources 196 (2011) 2241–2245.
[14] M. Nagahama, N. Hasegawa, S. Okada, J. Electrochem. Soc. 157 (2010) A748–A752.
[15] C. Frayret, A. Villesuzanne, N. Spaldin, E. Bousquet, J.N. Chotard, N. Recham, J.M. Tarascon, Phys. Chem. Chem. Phys. 12 (2010) 15512–15522.
[16] T. Mueller, G. Hautier, A. Jain, G. Ceder, Chem. Mater. 23 (2011) 3854–3862.
[17] Y. Cai, G. Chen, X. Xu, F. Du, Z. Li, X. Meng, C. Wang, Y. Wei, J. Phys. Chem. C 115 (2011) 7032–7037.
[18] R.C. Longo, K. Xiong, K. Cho, ECS Trans. 41 (2012) 75–85.
[19] Y. Xia, T. Sakai, T. Fujieda, M. Wada, H. Yoshinaga, Electrochem. Solid-State Lett. 4 (2001) A9–A11.
[20] C. Sigala, D. Guyomard, A. Verbaere, Y. Piffard, M. Tournoux, Solid State Ion. 81 (1995) 167–170.
[21] C. Sigala, A. Verbaere, J.L. Mansot, D. Guyomard, Y. Piffard, M. Tournoux, J. Solid State Chem. 132 (1997) 372–381.
[22] H. Kawai, M. Nagata, H. Kageyama, H. Tukamoto, A.R. West, Electrochim. Acta 45 (1999) 315–327.
[23] X. Huang, M. Lin, Q. Tong, X. Li, Y. Ruan, Y. Yang, J. Power Sources 202 (2012) 352–356.
[24] H. Kawai, M. Nagata, H. Tukamoto, A.R. West, J. Mater. Chem. 8 (1998) 837–839.
[25] H. Shigemura, M. Tabuchi, H. Kobayashi, H. Sakaebe, A. Hirano, H. Kageyama, J. Mater. Chem. 12 (2002) 1882–1891.
[26] H. Kawai, M. Nagata, M. Tabuchi, H. Tukamoto, A.R. West, Chem. Mater. 10 (1998) 3266–3268.
[27] Y. Ein-Eli, W.F. Howard, S.H. Lu, S. Mukerjee, J. McBreen, J.T. Vaughey, M.M. Thackeray, J. Electrochem. Soc. 145 (1998) 1238–1244.
[28] S. Mukerjee, X.Q. Yang, X. Sun, S.J. Lee, J. McBreen, Y. Ein-Eli, Electrochim. Acta 49 (2004) 3373–3382.
[29] Y. Shin, A. Manthiram, Electrochim. Acta 48 (2003) 3583–3592.
[30] Z. Lu, J.R. Dahn, J. Electrochem. Soc. 149 (2002) A815–A822.
[31] G.T.K. Fey, W. Li, J.R. Dahn, J. Electrochem. Soc. 141 (1994) 2279–2282.
[32] A.K. Padhi, K.S. Nanjundaswamy, J.B. Goodenough, J. Electrochem. Soc. 144 (1997) 1188–1194.
[33] A. Yamada, S.C. Chung, K. Hinokuma, J. Electrochem. Soc. 148 (2001) A224–A229.
[34] J. Liu, A. Manthiram, J. Electrochem. Soc. 156 (2009) A66–A72.
[35] J. Wolfenstine, J. Allen, J. Power Sources 136 (2004) 150–153.
[36] J. Gaubicher, C. Wurm, G. Goward, C. Masquelier, L. Nazar, Chem. Mater. 12 (2000) 3240–3242.
[37] P. Barpanda, S.-I. Nishimura, A. Yamada, Adv. Energy Mater. 2 (2012) 841–859.
[38] M. Dutreilh, C. Chevalier, M. El-Ghozzi, D. Avignant, J.M. Montel, J. Solid State Chem. 142 (1999) 1–5.
[39] S. Okada, M. Ueno, Y. Uebou, J.-I. Yamaki, J. Power Sources 146 (2005) 565–569.
[40] B.L. Ellis, W.R.M. Makahnouk, W.N. Rowan-Weetaluktuk, D.H. Ryan, L.F. Nazar, Chem. Mater. 22 (2010) 1059–1070.
[41] V. Legagneur, Y. An, A. Mosbah, R. Portal, A. Le Gal La Salle, A. Verbaere, D. Guyomard, Y. Piffard, Solid State Ion. 139 (2001) 37–46.
[42] N. Recham, J.N. Chotard, L. Dupont, C. Delacourt, W. Walker, M. Armand, J.M. Tarascon, Nat. Mater. 9 (2010) 68–74.
[43] T. Muraliganth, K.R. Stroukoff, A. Manthiram, Chem. Mater. 22 (2010) 5754–5761.
[44] K. Amine, H. Yasuda, M. Yamachi, Electrochem. Solid-State Lett. 3 (2000) 178–179.
[45] J. Wolfenstine, U. Lee, B. Poese, J.L. Allen, J. Power Sources 144 (2005) 226–230.
[46] F. Wang, J. Yang, Y. NuLi, J. Wang, J. Power Sources 195 (2010) 6884–6887.
[47] T. Muraliganth, A. Manthiram, J. Phys. Chem. C 114 (2010) 15530–15540.
[48] I. Taniguchi, T.N.L. Doan, B. Shao, Electrochim. Acta 56 (2011) 7680–7685.
[49] D.-W. Han, Y.-M. Kang, R.-Z. Yin, M.-S. Song, H.-S. Kwon, Electrochem. Commun. 11 (2009) 137–140.
[50] J.L. Allen, T.R. Jow, J. Wolfenstine, J. Power Sources 196 (2011) 8656–8661.
[51] Y. Zhang, C.S. Sun, Z. Zhou, Electrochem. Commun. 11 (2009) 1183–1186.
[52] N. Bramnik, K. Bramnik, T. Buhrmester, C. Baehtz, H. Ehrenberg, H. Fuess, J. Solid State Electrochem 8 (2004) 558–564.
[53] N.N. Bramnik, K.G. Bramnik, C. Baehtz, H. Ehrenberg, J. Power Sources 145 (2005) 74–81.
[54] M.E. Rabanal, M.C. Gutierrez, F. Garcia-Alvarado, E.C. Gonzalo, M.E. Arroyo-de Dompablo, J. Power Sources 160 (2006) 523–528.
[55] B. Jin, H.-B. Gu, K.-W. Kim, J. Solid State Electrochem. 12 (2007) 105–111.
[56] J. Wolfenstine, J. Read, J.L. Allen, J. Power Sources 163 (2007) 1070–1073.
[57] L. Tan, Z. Luo, H. Liu, Y. Yu, J. Alloys Compd. 502 (2010) 407–410.
[58] T.N.L. Doan, I. Taniguchi, J. Power Sources 196 (2011) 5679–5684.
[59] Q. Sun, J.-Y. Luo, Z.-W. Fu, Electrochem. Solid-State Lett. 14 (2011) A151–A153.
[60] J. Ni, H. Wang, L. Gao, L. Lu, Electrochim. Acta 70 (2012) 349–354.
[61] S.-M. Oh, S.-T. Myung, Y.-K. Sun, J. Mater. Chem. 22 (2012) 14932.
[62] J. Liu, T.E. Conry, X. Song, L. Yang, M.M. Doeff, T.J. Richardson, J. Mater. Chem. 21 (2011) 9984–9987.
[63] F. Wang, J. Yang, Y. NuLi, J. Wang, J. Power Sources 196 (2011) 4806–4810.
[64] I.C. Jang, H.H. Lim, S.B. Lee, K. Karthikeyan, V. Aravindan, K.S. Kang, W.S. Yoon, W.I. Cho, Y.S. Lee, J. Alloys Compd. 497 (2010) 321–324.

[65] J. Yang, J.J. Xu, J. Electrochem. Soc. 153 (2006) A716–A723.
[66] H. Ohkawa, K. Yoshida, M. Saito, K. Uematsu, K. Toda, M. Sato, Chem. Lett. (1999) 1017–1018.
[67] M.Y. Saïdi, J. Barker, H. Huang, J.L. Swoyer, G. Adamson, Electrochem. Solid-State Lett. 5 (2002) A149.
[68] C. Dai, Z. Chen, H. Jin, X. Hu, J. Power Sources 195 (2010) 5775–5779.
[69] J.S. Huang, L. Yang, K.Y. Liu, Y.F. Tang, J. Power Sources 195 (2010) 5013–5018.
[70] Y.Z. Dong, Y.M. Zhao, H. Duan, J. Electroanal. Chem. 660 (2011) 14–21.
[71] D. Ai, K. Liu, Z. Lu, M. Zou, D. Zeng, J. Ma, Electrochim. Acta 56 (2011) 2823–2827.
[72] A.R. Cho, J.N. Son, V. Aravindan, H. Kim, K.S. Kang, W.S. Yoon, W.S. Kim, Y.S. Lee, J. Mater. Chem. 22 (2012) 6556–6560.
[73] Y.G. Mateyshina, N.F. Uvarov, J. Power Sources 196 (2011) 1494–1497.
[74] C. Sun, S. Rajasekhara, Y. Dong, J.B. Goodenough, ACS Appl. Mater. Interfaces 3 (2011) 3772–3776.
[75] C. Deng, S. Zhang, S.Y. Yang, Y. Gao, B. Wu, L. Ma, B.L. Fu, Q. Wu, F.L. Liu, J. Phys. Chem. C 115 (2011) 15048–15056.
[76] Y. Chen, Y. Zhao, X. An, J. Liu, Y. Dong, L. Chen, Electrochim. Acta 54 (2009) 5844–5850.
[77] S.Y. Yang, S. Zhang, B.L. Fu, Q. Wu, F.L. Liu, C. Deng, J. Solid State Electrochem. 15 (2011) 2633–2638.
[78] M. Bini, S. Ferrari, D. Capsoni, V. Massarotti, Electrochim. Acta 56 (2011) 2648–2655.
[79] M. Ren, Z. Zhou, Y. Li, X.P. Gao, J. Yan, J. Power Sources 162 (2006) 1357–1362.
[80] Q. Kuang, Y. Zhao, X. An, J. Liu, Y. Dong, L. Chen, Electrochim. Acta 55 (2010) 1575–1581.
[81] L.-L. Zhang, X. Zhang, Y.-M. Sun, W. Luo, X.-L. Hu, X.-J. Wu, Y.-H. Huang, J. Electrochem. Soc. 158 (2011) A924–A929.
[82] J.H. Yao, S.S. Wei, P.J. Zhang, C.Q. Shen, K.F. Aguey-Zinsou, L.B. Wang, J. Alloys Compd. 532 (2012) 49–54.
[83] S. Zhang, Q. Wu, C. Deng, F.L. Liu, M. Zhang, F.L. Meng, H. Gao, J. Power Sources 218 (2012) 56–64.
[84] J. Yan, W. Yuan, Z.Y. Tang, H. Xie, W.F. Mao, L. Ma, J. Power Sources 209 (2012) 251–256.
[85] Y.Z. Li, X. Liu, J. Yan, Electrochim. Acta 53 (2007) 474–479.
[86] Y.Z. Li, Z. Zhou, X.P. Gao, J. Yan, Electrochim. Acta 52 (2007) 4922–4926.
[87] M.M. Ren, Z. Zhou, X.P. Gao, W.X. Peng, J.P. Wei, J. Phys. Chem. C 112 (2008) 5689–5693.
[88] Y.Z. Li, Z. Zhou, M.M. Ren, X.P. Gao, J. Yan, Electrochim. Acta 51 (2006) 6498–6502.
[89] Y. Li, Z. Zhou, X.P. Gao, J. Yan, J. Power Sources 160 (2006) 633–637.
[90] L. Zhang, H. Xiang, Z. Li, H. Wang, J. Power Sources 203 (2012) 121–125.
[91] H. Liu, P. Gao, J. Fang, G. Yang, Chem. Commun. 47 (2011) 9110–9112.
[92] H. Liu, G. Yang, X. Zhang, P. Gao, L. Wang, J. Fang, J. Pinto, X. Jiang, J. Mater. Chem. 22 (2012) 11039–11047.
[93] J. Zhai, M. Zhao, D. Wang, Y. Qiao, J. Alloys Compd. 502 (2010) 401–406.
[94] L.L. Zhang, G. Liang, G. Peng, F. Zou, Y.H. Huang, M.C. Croft, A. Ignatov, J. Phys. Chem. C 116 (2012) 12401–12408.
[95] S. Xun, J. Chong, X. Song, G. Liu, V.S. Battaglia, J. Mater. Chem. 22 (2012) 15775–15781.
[96] J. Hadermann, A.M. Abakumov, S. Turner, Z. Hafideddine, N.R. Khasanova, E.V. Antipov, G. Van Tendeloo, Chem. Mater. 23 (2011) 3540–3545.
[97] N.R. Khasanova, A.N. Gavrilov, E.V. Antipov, K.G. Bramnik, H. Hibst, J. Power Sources 196 (2011) 355–360.
[98] S. Amaresh, G.J. Kim, K. Karthikeyan, V. Aravindan, K.Y. Chung, B.W. Cho, Y.S. Lee, Phys. Chem. Chem. Phys. 14 (2012) 11904–11909.
[99] E. Dumont-Botto, C. Bourbon, S. Patoux, P. Rozier, M. Dolle, J. Power Sources 196 (2011) 2274–2278.
[100] J.H. Kim, S.T. Myung, C.S. Yoon, S.G. Kang, Y.K. Sun, Chem. Mater. 16 (2004) 906–914.
[101] D. Liu, J. Hamel-Paquet, J. Trottier, F. Barray, V. Gariépy, P. Hovington, A. Guerfi, A. Mauger, C.M. Julien, J.B. Goodenough, K. Zaghib, J. Power Sources 217 (2012) 400–406.
[102] Q. Zhong, A. Bonakdarpour, M. Zhang, Y. Gao, J.R. Dahn, J. Electrochem. Soc. 144 (1997) 205–213.
[103] R. Alcántara, M. Jaraba, P. Lavela, J.L. Tirado, P. Biensan, A. de Guibert, C. Jordy, J.P. Peres, Chem. Mater. 15 (2003) 2376–2382.
[104] J. Song, D.W. Shin, Y. Lu, C.D. Amos, A. Manthiram, J.B. Goodenough, Chem. Mater. 24 (2012) 3101–3109.
[105] H. Wang, T.A. Tan, P. Yang, M.O. Lai, L. Lu, J. Phys. Chem. C 115 (2011) 6102–6110.
[106] D. Liu, Y. Lu, J.B. Goodenough, J. Electrochem. Soc. 157 (2010) A1269–A1273.
[107] M. Aklalouch, J.M. Amarilla, R.M. Rojas, I. Saadoune, J.M. Rojo, Electrochem. Commun. 12 (2010) 548–552.
[108] M. Aklalouch, J.M. Amarilla, R.M. Rojas, I. Saadoune, J.M. Rojo, J. Power Sources 185 (2008) 501–511.
[109] C. Locati, U. Lafont, L. Simonin, F. Ooms, E.M. Kelder, J. Power Sources 174 (2007) 847–851.
[110] G.B. Zhong, Y.Y. Wang, Y.Q. Yu, C.H. Chen, J. Power Sources 205 (2012) 385–393.
[111] J. Liu, A. Manthiram, J. Phys. Chem. C 113 (2009) 15073–15079.
[112] N. Kawai, T. Nakamura, Y. Yamada, M. Tabuchi, J. Power Sources 196 (2011) 6969–6973.
[113] S.H. Oh, S.H. Jeon, W.I. Cho, C.S. Kim, B.W. Cho, J. Alloys Compd. 452 (2008) 389–396.
[114] M.-C. Yang, B. Xu, J.-H. Cheng, C.-J. Pan, B.-J. Hwang, Y.S. Meng, Chem. Mater. 23 (2011) 2832–2841.
[115] T.-F. Yi, Y. Xie, Y.-R. Zhu, R.-S. Zhu, M.-F. Ye, J. Power Sources 211 (2012) 59–65.
[116] D.W. Shin, C.A. Bridges, A. Huq, M.P. Paranthaman, A. Manthiram, Chem. Mater. 24 (2012) 3720–3731.
[117] X.X. Xu, J. Yang, Y.Q. Wang, Y.N. NuLi, J.L. Wang, J. Power Sources 174 (2007) 1113–1116.
[118] S.-W. Oh, S.-H. Park, J.-H. Kim, Y.C. Bae, Y.-K. Sun, J. Power Sources 157 (2006) 464–470.
[119] J.C. Arrebola, A. Caballero, L. Hernán, J. Morales, J. Power Sources 195 (2010) 4278–4284.
[120] Y.K. Sun, C.S. Yoon, I.H. Oh, Electrochim. Acta 48 (2003) 503–506.
[121] Y.-K. Sun, K.-J. Hong, Jai Prakash, K. Amine, Electrochem. Commun. 4 (2002) 344–348.
[122] J. Liu, A. Manthiram, Chem. Mater. 21 (2009) 1695–1707.
[123] H.-B. Kang, S.-T. Myung, K. Amine, S.-M. Lee, Y.-K. Sun, J. Power Sources 195 (2010) 2023–2028.
[124] J. Liu, A. Manthiram, J. Electrochem. Soc. 156 (2009) A833–A838.
[125] T. Noguchi, I. Yamazaki, T. Numata, M. Shirakata, J. Power Sources 174 (2007) 359–365.
[126] Y. Fan, J. Wang, Z. Tang, W. He, J. Zhang, Electrochim. Acta 52 (2007) 3870–3875.
[127] H.M. Wu, I. Belharouak, A. Abouimrane, Y.K. Sun, K. Amine, J. Power Sources 195 (2010) 2909–2913.
[128] G. Zhao, Y. Lin, T. Zhou, Y. Lin, Y. Huang, Z. Huang, J. Power Sources 215 (2012) 63–68.
[129] Y. Kobayashi, H. Miyashiro, K. Takei, H. Shigemura, M. Tabuchi, H. Kageyama, T. Iwahori, J. Electrochem. Soc. 150 (2003) A1577–A1582.
[130] J. Chong, S. Xun, X. Song, G. Liu, V.S. Battaglia, Nano Energy 2 (2013) 283–293.
[131] J.Y. Shi, C.-W. Yi, K. Kim, J. Power Sources 195 (2010) 6860–6866.
[132] D. Liu, Y. Bai, S. Zhao, W. Zhang, J. Power Sources 219 (2012) 333–338.
[133] D. Liu, J. Trottier, P. Charest, J. Fréchette, A. Guerfi, A. Mauger, C.M. Julien, K. Zaghib, J. Power Sources 204 (2012) 127–132.
[134] J. Arrebola, A. Caballero, L. Hernán, J. Morales, E. Rodríguez Castellón, Electrochem. Solid-State Lett. 8 (2005) A303–A307.
[135] J. Arrebola, A. Caballero, L. Hernán, J. Morales, E. Rodríguez Castellón, J.R. Ramos Barrado, J. Electrochem. Soc. 154 (2007) A178–A184.
[136] T. Yang, N. Zhang, Y. Lang, K. Sun, Electrochim. Acta 56 (2011) 4058–4064.
[137] J.-H. Cho, J.-H. Park, M.-H. Lee, H.-K. Song, S.-Y. Lee, Energy Environ. Sci. 5 (2012) 7124–7131.
[138] K.M. Shaju, P.G. Bruce, Dalton Trans. (2008) 5471–5475.
[139] Z. Chen, S. Qiu, Y. Cao, X. Ai, K. Xie, X. Hong, H. Yang, J. Mater. Chem. 22 (2012) 17768.
[140] M.S. Song, A. Benayad, Y.M. Choi, K.S. Park, Chem. Commun. 48 (2011) 516–518.
[141] H.-G. Jung, S.-T. Myung, C.S. Yoon, S.-B. Son, K.H. Oh, K. Amine, B. Scrosati, Y.-K. Sun, Energy Environ. Sci. 4 (2011) 1345–1351.
[142] Y. Tang, F. Huang, W. Zhao, Z. Liu, D. Wan, J. Mater. Chem. 22 (2012) 11257–11260.
[143] E. Ferg, R.J. Gummow, A. de Kock, M.M. Thackeray, J. Electrochem. Soc. 141 (1994) L147–L150.
[144] L. Aldon, P. Kubiak, M. Womes, J.C. Jumas, J. Olivier-Fourcade, J.L. Tirado, J.I. Corredor, C. Pérez Vicente, Chem. Mater. 16 (2004) 5721–5725.
[145] H.G. Jung, M.W. Jang, J. Hassoun, Y.K. Sun, B. Scrosati, Nat. Commun. 2 (2011) 516–520.
[146] S. Brutti, V. Gentili, P. Reale, L. Carbone, S. Panero, J. Power Sources 196 (2011) 9792–9799.
[147] J.-T. Han, J.B. Goodenough, Chem. Mater. 23 (2011) 3404–3407.
[148] J.C. Arrebola, A. Caballero, L. Hernán, J. Morales, J. Power Sources 183 (2008) 310–315.
[149] J.C. Arrebola, A. Caballero, J.L. Gómez-Cámer, L. Hernán, J. Morales, L. Sánchez, Electrochem. Commun. 11 (2009) 1061–1064.
[150] J. Hassoun, G. Derrien, S. Panero, B. Scrosati, Adv. Mater. 20 (2008) 3169–3175.
[151] J. Hassoun, K.-S. Lee, Y.-K. Sun, B. Scrosati, J. Am. Chem. Soc. 133 (2011) 3139–3143.
[152] J. Hassoun, P. Reale, S. Panero, B. Scrosati, M. Wachtler, M. Fleischhammer, M. Kasper, M. Wohlfahrt-Mehrens, Electrochim. Acta 55 (2010) 4194–4200.
[153] Y.K. Sun, S.T. Myung, B.C. Park, J. Prakash, I. Belharouak, K. Amine, Nat. Mater. 8 (2009) 320–324.
[154] K.A. Jarvis, Z.Q. Deng, L.F. Allard, A. Manthiram, P.J. Ferreira, Chem. Mater. 23 (2011) 3614–3621.
[155] J. Bareno, M. Balasubramanian, S.H. Kang, J.G. Wen, C.H. Lei, S.V. Pol, I. Petrov, D.P. Abraham, Chem. Mater. 23 (2011) 2039–2050.
[156] J. Bareno, C.H. Lei, J.G. Wen, S.H. Kang, I. Petrov, D.P. Abraham, Adv. Mater. 22 (2010) 1122–1127.
[157] M. Oishi, T. Fujimoto, Y. Takanashi, Y. Orikasa, A. Kawamura, T. Ina, H. Yamashige, D. Takamatsu, K. Sato, H. Murayama, H. Tanida, H. Arai, H. Ishii, C. Yogi, I. Watanabe, T. Ohta, A. Mineshige, Y. Uchimoto, Z. Ogumi, J. Power Sources 222 (2013) 45–51.
[158] N. Yabuuchi, K. Yoshii, S.T. Myung, I. Nakai, S. Komaba, J. Am. Chem. Soc. 133 (2011) 4404–4419.

[159] M. Gu, I. Belharouak, J. Zheng, H. Wu, J. Xiao, A. Genc, K. Amine, S. Thevuthasan, D.R. Baer, J.G. Zhang, N.D. Browning, J. Liu, C. Wang, ACS Nano 7 (2013) 760–767.
[160] D. Mohanty, S. Kalnaus, R.A. Meisner, K.J. Rhodes, J. Li, E.A. Payzant, D.L. Wood, C. Daniel, J. Power Sources 229 (2013) 239–248.
[161] A. Boulineau, L. Simonin, J.-F. Colin, E. Canévet, L. Daniel, S. Patoux, Chem. Mater. 24 (2012) 3558–3566.
[162] B. Xu, C.R. Fell, M. Chi, Y.S. Meng, Energy Environ. Sci. 4 (2011) 2223–2233.
[163] C.S. Johnson, N. Li, C. Lefief, J.T. Vaughey, M.M. Thackeray, Chem. Mater. 20 (2008) 6095–6106.
[164] C.S. Johnson, J.S. Kim, C. Lefief, N. Li, J.T. Vaughey, M.M. Thackeray, Electrochem. Commun. 6 (2004) 1085–1091.
[165] J.S. Kim, C.S. Johnson, J.T. Vaughey, M.M. Thackeray, J. Power Sources 153 (2006) 258–264.
[166] J. Zheng, S. Deng, Z. Shi, H. Xu, H. Xu, Y. Deng, Z. Zhang, G. Chen, J. Power Sources 221 (2013) 108–113.
[167] D.Y.W. Yu, K. Yanagida, H. Nakamura, J. Electrochem. Soc. 157 (2010) A1177–A1182.
[168] J. Gao, J. Kim, A. Manthiram, Electrochem. Commun. 11 (2009) 84–86.
[169] J. Gao, A. Manthiram, J. Power Sources 191 (2009) 644–647.
[170] H. Yu, H. Zhou, J. Mater. Chem. 22 (2012) 15507–15510.
[171] S.H. Kang, M.M. Thackeray, J. Electrochem. Soc. 155 (2008) A269–A275.
[172] J.M. Zheng, Z.R. Zhang, X.B. Wu, Z.X. Dong, Z. Zhu, Y. Yang, J. Electrochem. Soc. 155 (2008) A775–A782.
[173] S.K. Martha, J. Nanda, G.M. Veith, N.J. Dudney, J. Power Sources 216 (2012) 179–186.
[174] J. Liu, Q. Wang, B. Reeja-Jayan, A. Manthiram, Electrochem. Commun. 12 (2010) 750–753.
[175] J.-H. Kim, M.-S. Park, J.-H. Song, D.-J. Byun, Y.-J. Kim, J.-S. Kim, J. Alloys Compd. 517 (2012) 20–25.
[176] C. Wu, X. Fang, X. Guo, Y. Mao, J. Ma, C. Zhao, Z. Wang, L. Chen, J. Power Sources 231 (2013) 44–49.
[177] G. Singh, R. Thomas, A. Kumar, R.S. Katiyar, A. Manivannan, J. Electrochem. Soc. 159 (2012) A470–A478.
[178] Y.J. Kang, J.H. Kim, S.W. Lee, Y.K. Sun, Electrochim. Acta 50 (2005) 4784–4791.
[179] G.R. Li, X. Feng, Y. Ding, S.H. Ye, X.P. Gao, Electrochim. Acta 78 (2012) 308–315.
[180] W.C. West, J. Soler, M.C. Smart, B.V. Ratnakumar, S. Firdosy, V. Ravi, M.S. Anderson, J. Hrbacek, E.S. Lee, A. Manthiram, J. Electrochem. Soc. 158 (2011) A883–A889.
[181] D. Shin, C. Wolverton, J.R. Croy, M. Balasubramanian, S.H. Kang, C.M.L. Rivera, M.M. Thackeray, J. Electrochem. Soc. 159 (2012) A121–A127.
[182] S.-H. Kang, M.M. Thackeray, Electrochem. Commun. 11 (2009) 748–751.
[183] H.Z. Zhang, Q.Q. Qiao, G.R. Li, S.H. Ye, X.P. Gao, J. Mater. Chem. 22 (2012) 13104–13109.
[184] K.J. Rosina, M. Jiang, D. Zeng, E. Salager, A.S. Best, C.P. Grey, J. Mater. Chem. 22 (2012) 20602–20610.
[185] M. Bettge, Y. Li, B. Sankaran, N.D. Rago, T. Spila, R.T. Haasch, I. Petrov, D.P. Abraham, J. Power Sources 233 (2013) 346–357.
[186] Y. Wu, A. Manthiram, Solid State Ion. 180 (2009) 50–56.
[187] W. He, J. Qian, Y. Cao, X. Ai, H. Yang, RSC Adv. 2 (2012) 3423–3429.
[188] Y. Wu, A. Vadivel Murugan, A. Manthiram, J. Electrochem. Soc. 155 (2008) A635–A641.
[189] Y.K. Sun, M.J. Lee, C.S. Yoon, J. Hassoun, K. Amine, B. Scrosati, Adv. Mater. 24 (2012) 1192–1196.
[190] G. Singh, R. Thomas, A. Kumar, R.S. Katiyar, J. Electrochem. Soc. 159 (2012) A410–A420.
[191] Z.Q. Deng, A. Manthiram, J. Phys. Chem. C 115 (2011) 7097–7103.
[192] S.-W. Cho, G.-O. Kim, K.-S. Ryu, Solid State Ion. 206 (2012) 84–90.
[193] K. Xu, Chem. Rev. 104 (2004) 4303–4418.
[194] K. Xu, S.P. Ding, T.R. Jow, J. Electrochem. Soc. 146 (1999) 4172–4178.
[195] A. Lewandowski, A. Świderska-Mocek, J. Power Sources 194 (2009) 601–609.
[196] H. Matsumoto, H. Sakaebe, K. Tatsumi, J. Power Sources 146 (2005) 45–50.
[197] H. Sakaebe, H. Matsumoto, Electrochem. Commun. 5 (2003) 594–598.
[198] M. Galiński, A. Lewandowski, I. Stępniak, Electrochim. Acta 51 (2006) 5567–5580.
[199] V. Borgel, E. Markevich, D. Aurbach, G. Semrau, M. Schmidt, J. Power Sources 189 (2009) 331–336.
[200] J. Mun, T. Yim, K. Park, J.H. Ryu, Y.G. Kim, S.M. Oh, J. Electrochem. Soc. 158 (2011) A453–A457.
[201] A. Guerfi, M. Dontigny, P. Charest, M. Petitclerc, M. Lagacé, A. Vijh, K. Zaghib, J. Power Sources 195 (2010) 845–852.
[202] J. Xiang, F. Wu, R. Chen, L. Li, H. Yu, J. Power Sources 233 (2013) 115–120.
[203] R.S. Kühnel, N. Böckenfeld, S. Passerini, M. Winter, A. Balducci, Electrochim. Acta 56 (2011) 4092–4099.
[204] H.F. Xiang, B. Yin, H. Wang, H.W. Lin, X.W. Ge, S. Xie, C.H. Chen, Electrochim. Acta 55 (2010) 5204–5209.
[205] J. Jin, H.H. Li, J.P. Wei, X.K. Bian, Z. Zhou, J. Yan, Electrochem. Commun. 11 (2009) 1500–1503.
[206] H. Sano, H. Sakaebe, H. Matsumoto, J. Electrochem. Soc. 158 (2011) A316–A321.
[207] K. Xu, C.A. Angell, J. Electrochem. Soc. 149 (2002) A920–A926.
[208] N. Shao, X.G. Sun, S. Dai, D.E. Jiang, J. Phys. Chem. B 115 (2011) 12120–12125.
[209] K. Xu, C.A. Angell, J. Electrochem. Soc. 145 (1998) L70–L72.
[210] N. Shao, X.G. Sun, S. Dai, D.E. Jiang, J. Phys. Chem. B 116 (2012) 3235–3238.
[211] X.-G. Sun, C.A. Angell, Electrochem. Commun. 7 (2005) 261–266.
[212] Y. Watanabe, S.-I. Kinoshita, S. Wada, K. Hoshino, H. Morimoto, S.-I. Tobishima, J. Power Sources 179 (2008) 770–779.
[213] X. Sun, C.A. Angell, 213th ECS Meeting Abstracts MA2008-01, 2008, 162.
[214] S. Li, W. Zhao, X. Cui, Y. Zhao, B. Li, H. Zhang, Y. Li, G. Li, X. Ye, Y. Luo, Electrochim. Acta 91 (2013) 282–292.
[215] F. Wu, J. Xiang, L. Li, J. Chen, G. Tan, R. Chen, J. Power Sources 202 (2012) 322–331.
[216] F. Wu, Q. Zhu, L. Li, R. Chen, S. Chen, J. Mater. Chem. A 1 (2013) 3659–3666.
[217] H. Fang, H. Yi, C. Hu, B. Yang, Y. Yao, W. Ma, Y. Dai, Electrochim. Acta 71 (2012) 266–269.
[218] A. Abouimrane, I. Belharouak, K. Amine, Electrochem. Commun. 11 (2009) 1073–1076.
[219] L. Mao, B. Li, X. Cui, Y. Zhao, X. Xu, X. Shi, S. Li, F. Li, Electrochim. Acta 79 (2012) 197–201.
[220] S.-Y. Lee, K. Ueno, C.A. Angell, J. Phys. Chem. C 116 (2012) 23915–23920.
[221] L. Xing, J. Vatamanu, O. Borodin, G.D. Smith, D. Bedrov, J. Phys. Chem. C 116 (2012) 23871–23881.
[222] X. Sun, C.A. Angell, Electrochem. Commun. 11 (2009) 1418–1421.
[223] M. Ue, K. Ida, S. Mori, J. Electrochem. Soc. 141 (1994) 2989–2996.
[224] M. Ue, M. Takeda, M. Takehara, S. Mori, J. Electrochem. Soc. 144 (1997) 2684–2688.
[225] Y. Abu-Lebdeh, I. Davidson, J. Electrochem. Soc. 156 (2009) A60–A65.
[226] Y. Abu-Lebdeh, I. Davidson, J. Power Sources 189 (2009) 576–579.
[227] B. Oh, D. Ofer, J. Rempel, S. Sriramulu, B. Barnett, 218th ECS Meeting Abstracts MA2010-02, 2010, 592.
[228] A.J. Gmitter, I. Plitz, G.G. Amatucci, J. Electrochem. Soc. 159 (2012) A370–A379.
[229] R. McMillan, H. Slegr, Z.X. Shu, W. Wang, J. Power Sources 81-82 (1999) 20–26.
[230] P.M. Le, F. Alloin, P. Strobel, A. Moussa, B. Langlois, 219th ECS Meeting Abstracts MA2011-01, 2011, 382.
[231] D. Kobayashi, M. Takehara, N. Nanbu, M. Ue, Y. Sasaki, 214th ECS Meeting Abstracts MA2008-02, 2008, 166.
[232] R. Sharabi, E. Markevich, K. Fridman, G. Gershinsky, G. Salitra, D. Aurbach, G. Semrau, M.A. Schmidt, N. Schall, C. Bruenig, Electrochem. Commun. 28 (2013) 20–23.
[233] G.G. Amatucci, J.M. Tarascon, L.C. Klein, J. Electrochem. Soc. 143 (1996) 1114–1123.
[234] T. Kitagawa, K. Azuma, M. Koh, A. Yamauchi, M. Kagawa, H. Sakata, H. Miyawaki, A. Nakazono, H. Arima, M. Yamagata, M. Ishikawa, Electrochemistry 78 (2010) 345–348.
[235] G.H. Wrodnigg, J.O. Besenhard, M. Winter, J. Electrochem. Soc. 146 (1999) 470–472.
[236] C.-C. Chang, L.-J. Her, L.-C. Chen, Y.-Y. Lee, S.-J. Liu, H.-J. Tien, J. Power Sources 163 (2007) 1059–1063.
[237] W. Yao, Z. Zhang, J. Gao, J. Li, J. Xu, Z. Wang, Y. Yang, Energy Environ. Sci. 2 (2009) 1102–1108.
[238] L. Yang, B. Ravdel, B.L. Lucht, Electrochem. Solid-State Lett. 13 (2010) A95–A97.
[239] W. Xu, J. Xiao, X. Chen, F. Ding, D. Wang, A. Pan, J.-G. Zhang, 220th Meeting Abstracts MA2011-02, 2011, 1265.
[240] V. Aravindan, Y.L. Cheah, W.C. Ling, S. Madhavi, J. Electrochem. Soc. 159 (2012) A1435–A1439.
[241] S. Dalavi, M. Xu, B. Knight, B.L. Lucht, Electrochem. Solid-State Lett. 15 (2012) A28–A31.
[242] K. Xu, U. Lee, S.S. Zhang, T.R. Jow, J. Electrochem. Soc. 151 (2004) A2106–A2112.
[243] K. Xu, S. Zhang, R. Jow, J. Power Sources 143 (2005) 197–202.
[244] Q. Wu, W. Lu, M. Miranda, T.K. Honaker-Schroeder, K.Y. Lakhsassi, D. Dees, Electrochem. Commun. 24 (2012) 78–81.
[245] Y. Zhu, Y. Li, M. Bettge, D.P. Abraham, J. Electrochem. Soc. 159 (2012) A2109–A2117.
[246] M. Hu, J. Wei, L. Xing, Z. Zhou, J. Appl. Electrochem. 42 (2012) 291–296.
[247] L. Yang, T. Markmaitree, B.L. Lucht, J. Power Sources 196 (2011) 2251–2254.
[248] L. Yang, B.L. Lucht, Electrochem. Solid-State Lett. 12 (2009) A229–A231.
[249] M. Xu, Y. Liu, B. Li, W. Li, X. Li, S. Hu, Electrochem. Commun. 18 (2012) 123–126.
[250] A. von Cresce, K. Xu, J. Electrochem. Soc. 158 (2011) A337–A342.
[251] J.-N. Lee, G.-B. Han, M.-H. Ryou, D.J. Lee, S. Jongchan, J.W. Choi, J.-K. Park, Electrochim. Acta 56 (2011) 5195–5200.
[252] X. Zuo, C. Fan, X. Xiao, J. Liu, J. Nan, J. Power Sources 219 (2012) 94–99.
[253] Z. Wang, N. Dupre, L. Lajaunie, P. Moreau, J.-F. Martin, L. Boutafa, S. Patoux, D. Guyomard, J. Power Sources 215 (2012) 170–178.
[254] V. Tarnopolskiy, J. Kalhoff, M. Nádherná, D. Bresser, L. Picard, F. Fabre, M. Rey, S. Passerini, J. Power Sources 236 (2013) 39–46.
[255] T. Kubota, M. Ihara, S. Katayama, H. Nakai, J. Ichikawa, J. Power Sources 207 (2012) 141–149.
[256] H. Lee, S. Choi, S. Choi, H.-J. Kim, Y. Choi, S. Yoon, J.-J. Cho, Electrochem. Commun. 9 (2007) 801–806.
[257] T. Horino, H. Tamada, A. Kishimoto, J. Kaneko, Y. Iriyama, Y. Tanaka, T. Fujinami, J. Electrochem. Soc. 157 (2010) A677–A681.
[258] H.-C. Wu, C.-Y. Su, D.-T. Shieh, M.-H. Yang, N.-L. Wu, Electrochem. Solid-State Lett. 9 (2006) A537–A541.

[259] L. El Ouatani, R. Dedryvére, C. Siret, P. Biensan, S. Reynaud, P. Iratçabal, D. Gonbeau, J. Electrochem. Soc. 156 (2009) A103–A113.
[260] J.-Y. Eom, I.-H. Jung, J.-H. Lee, J. Power Sources 196 (2011) 9810–9814.
[261] K. Abe, Y. Ushigoe, H. Yoshitake, M. Yoshio, J. Power Sources 153 (2006) 328–335.
[262] T. Takeuchi, T. Kyuna, H. Morimoto, S.-i. Tobishima, J. Power Sources 196 (2011) 2790–2801.
[263] M. Hu, J. Wei, L. Xing, Z. Zhou, J. Power Sources 222 (2013) 373–378.
[264] L.Y. Xing, M. Hu, Q. Tang, J.P. Wei, X. Qin, Z. Zhou, Electrochim. Acta 59 (2012) 172–178.
[265] K.-S. Lee, Y.-K. Sun, J. Noh, K.S. Song, D.-W. Kim, Electrochem. Commun. 11 (2009) 1900–1903.
[266] Y.-S. Lee, K.-S. Lee, Y.-K. Sun, Y.M. Lee, D.-W. Kim, J. Power Sources 196 (2011) 6997–7001.
[267] A. Abouimrane, S.A. Odom, H. Tavassol, M.V. Schulmerich, H. Wu, R. Bhargava, A.A. Gewirth, J.S. Moore, K. Amine, J. Electrochem. Soc. 160 (2012) A268–A271.
[268] J. Zheng, J. Xiao, W. Xu, X. Chen, M. Gu, X. Li, J.-G. Zhang, J. Power Sources 227 (2013) 211–217.
[269] J. Li, R. Klöpsch, S. Nowak, M. Kunze, M. Winter, S. Passerini, J. Power Sources 196 (2011) 7687–7691.
[270] J. Xu, S.-L. Chou, Q.-F. Gu, H.-K. Liu, S.-X. Dou, J. Power Sources 225 (2013) 172–178.
[271] N.N. Sinha, J.C. Burns, R.J. Sanderson, J. Dahn, J. Electrochem. Soc. 158 (2011) A1400–A1403.
[272] R. Sharabi, E. Markevich, V. Borgel, G. Salitra, D. Aurbach, G. Semrau, M.A. Schmidt, N. Schall, C. Stinner, Electrochem. Commun. 13 (2011) 800–802.
[273] K.W. Leitner, H. Wolf, A. Garsuch, F. Chesneau, M. Schulz-Dobrick, J. Power Sources (2013), http://dx.doi.org/10.1016/j.jpowsour.2013.01.187.
[274] X. Chen, W. Xu, J. Xiao, M.H. Engelhard, F. Ding, D. Mei, D. Hu, J. Zhang, J.-G. Zhang, J. Power Sources 213 (2012) 160–168.
[275] H. Duncan, Y. Abu-Lebdeh, I.J. Davidson, J. Electrochem. Soc. 157 (2010) A528–A535.
[276] H.F. Xiang, Q.Y. Jin, R. Wang, C.H. Chen, X.W. Ge, J. Power Sources 179 (2008) 351–356.
[277] L. Zhang, Z. Zhang, H. Wu, K. Amine, Energy Environ. Sci. 4 (2011) 2858–2862.
[278] Y.-K. Han, J. Jung, S. Yu, H. Lee, J. Power Sources 187 (2009) 581–585.